AD-A058 380 GENERAL ELECTRIC CO WILMINGTON MASS F/G 10/2
EVALUATION AND OPTIMIZATION OF SOLID POLYMER ELECTROLYTE (SPE) --ETC(U)
MAY 78 E N MACLEOD, J F MCELROY DAAK70-77-C-0128
UNCLASSIFIED MPR-022 NL

1 OF 1
AD
A058 380

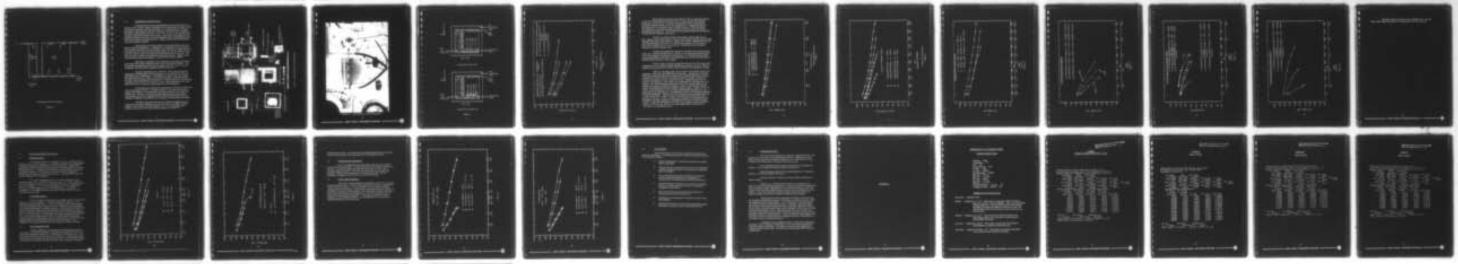

END
DATE
FILMED
-11-78
DDC

AIRCRAFT EQUIPMENT DIVISION

MPR-022
May 15, 1978

(12) LEVEL II

REPORT

EVALUATION AND OPTIMIZATION OF SOLID POLYMER ELECTROLYTE (SPE) FUEL CELLS

Final Technical Program
Report
May 23, 1977 through April 23, 1978
Contract DAAK 70-77-C-0128
DRL Line Item No. 002
Prepared for
Army Mobility Equipment - Research and Development Command
Fort Belvoir, Virginia 22060

DIRECT ENERGY CONVERSION PROGRAMS
50 FORDHAM ROAD
WILMINGTON, MASSACHUSETTS 01887

GENERAL ELECTRIC

389 779

AIRCRAFT EQUIPMENT DIVISION

MPR-022
May 15, 1978

REPORT

EVALUATION AND OPTIMIZATION OF SOLID POLYMER ELECTROLYTE (SPE) FUEL CELLS

Final Technical Program

Report

May 23, 1977 through April 23, 1978

Contract DAAK 70-77-C-0128

DRL Line Item No. 002

Prepared for

Army Mobility Equipment - Research and Development Command

Fort Belvoir, Virginia 22060

DIRECT ENERGY CONVERSION PROGRAMS
50 FORDHAM ROAD
WILMINGTON, MASSACHUSETTS 01887

78 08 24 002

GENERAL ELECTRIC

DISTRIBUTION STATEMENT A
Approved for public release;
Distribution Unlimited

NOTICES

AVAILABILITY

~~This document is subject to special export controls and each transmittal to foreign governments or foreign nationals may be made only with prior approval of Army Mobility Equipment-Research and Development Command, Fort Belvoir, Virginia 22060.~~

DISCLAIMERS

DISPOSITION

SECURITY CLASSIFICATION OF THIS PAGE (When Data Entered)

REPORT DOCUMENTATION PAGE	READ INSTRUCTIONS BEFORE COMPLETING FORM
1. REPORT NUMBER MPR-022 ? — 2. GOVT ACCESSION NO.	3. RECIPIENT'S CATALOG NUMBER
4. TITLE (and Subtitle) (6) Evaluation and Optimization of Solid Polymer Electrolyte (SPE) Fuel Cells,	5. TYPE OF REPORT & PERIOD COVERED Final Technical Report May 23, 1977 thru April 23, 1978
	6. PERFORMING ORG. REPORT NUMBER
7. AUTHOR(s) (10) Edward N. MacLeod [redacted] James F. McElroy	8. CONTRACT OR GRANT NUMBER(s) (15) DAAK 70-77-C-0128
9. PERFORMING ORGANIZATION NAME AND ADDRESS Direct Energy Conversion Programs General Electric Company 50 Fordham Road; Wilmington, MA 01887	10. PROGRAM ELEMENT, PROJECT, TASK AREA & WORK UNIT NUMBERS A321/E74/7 7A 320330
11. CONTROLLING OFFICE NAME AND ADDRESS DCAS PRO General Electric Company 1100 Western Avenue; Lynn, MA 01910	12. REPORT DATE May 15, 1978
	13. NUMBER OF PAGES 39
14. MONITORING AGENCY NAME & ADDRESS(if different from Controlling Office) Army Mobility Equipment - Research And Development Command Fort Belvoir, Virginia 22060	15. SECURITY CLASS. (of this report) Unclassified
	15a. DECLASSIFICATION/DOWNGRADING SCHEDULE

16. DISTRIBUTION STATEMENT (of this Report)

This document has been approved for public release and sale. Its distribution is unlimited.

(11) 15 May 78 (14) MPR-022

17. DISTRIBUTION STATEMENT (of the abstract entered in Block 20, if different from Report)

Approved for public release. (12) 45p.

18. SUPPLEMENTARY NOTES

(9) Final technical rept. 23 May 77-23 Apr 78,

19. KEY WORDS (Continue on reverse side if necessary and identify by block number)

Fuel Cells	Methanol
Solid Polymer Electrolyte (SPE)	Humidification
Reformate	

20. ABSTRACT (Continue on reverse side if necessary and identify by block number)

The reaction air of a fuel/air solid polymer electrolyte (SPE) fuel cell was water saturated utilizing excess moisture in the fuel by diffusion thru an uncatalized portion of the SPE. This device eliminated the need for external humidification controls. Fuel/air current densities up to 750 ma/cm^2 were demonstrated.

SQ CM

DD FORM 1 JAN 73 1473 EDITION OF 1 NOV 65 IS OBSOLETE

UNCLASSIFIED

SECURITY CLASSIFICATION OF THIS PAGE (When Data Entered)

389 779

ACKNOWLEDGMENTS

This report summarizes the results of a Solid Polymer Electrolyte fuel cell technology program conducted for the Army Mobility Equipment - Research and Development Command (MERADCOM) Fort Belvoir, Virginia, by the General Electric Company, Direct Energy Conversion Programs, Wilmington, Massachusetts, under Contract DAAK 70-77-C-0128. The period of performance was May 23, 1977 through April 23, 1978.

This work was performed under the guidance of Mr. W.G. Taschek, Technical Representative, Electrochemical Division, Power Systems Group MERADCOM. The overall program was directed by J.F. McElroy, Project Engineer, General Electric Company, Direct Energy Conversion Programs.

Delete NOFORN Statement per Mr. W. G. Taschek, AMERDC

CONTENTS

1.0 SUMMARY

This final technical report reviews work performed under Army Mobility Equipment Research and Development Command (MERADCOM) Contract DAAK-70-77-C-0128 during the period May 23, 1977 through April 23, 1978.

The advantages of electrochemical power generation derived from an easily transportable fuel such as methanol have long been recognized. Military and commercial concerns alike could make considerable use of such a development.

The objective of this effort has been to design, fabricate and test evaluate Solid Polymer Electrolyte (SPE) fuel cell configurations suitable for operation on reformed methanol and air. A major thrust of this program was the development of a configuration that internally humidified the reactive air. In this regard the expertise gained through development of a Solid Polymer reactant humidifier for NASA/JSC (Contract NAS 9-12332) was of considerable benefit. In order to simulate the fuel and excess water delivered from a methanol reformer, a water injection mechanism was employed at the fuel inlet to the fuel cell. This injected water was utilized for air humidification. During the course of this contract, laboratory-sized cells were developed and successfully operated on simulated methanol reformate and air with internal humidification. Environmental and overstress testing was also successfully completed. Figure 1 reflects the various tasks performed during the course of the contract.

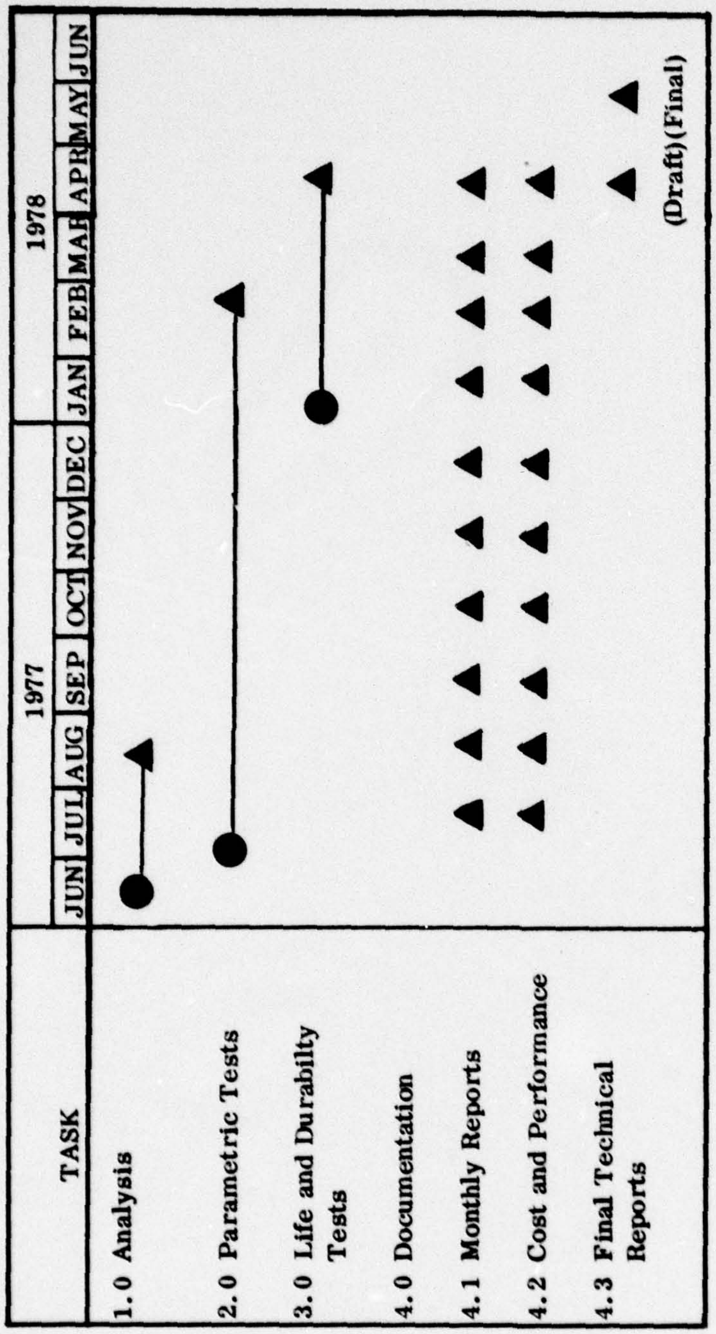

Figure 1. Proposed Program Milestone Chart

2.0 ANALYSIS (Task 1.0)

The overall purpose of the analysis task was to determine area ratios of humidification SPE to electrochemically active SPE at various operating conditions. Establishment of the anode side water introduction technique to simulate excess reformer water was also to be accomplished.

Previous computer subroutines involving mass transport, current densities, partial pressures, SPE thickness, IEC (Ion Exchange Capacity), etc., were use to obtain a mathematical model of a self-humidifying configuration.

Operational conditions utilized in the NASA/JSC Program were factored into the computer program for a comparison with humidifier area-to-active area ratios as established for the near-ambient pressure cell.

These analyses produced a humidifier area of 1.02 in^2 for the 165°F case. Using a fixed area ratio (i.e., 14% area for humidification) the required operating pressures were determined for proper humidification at higher temperatures. Table I reflects the range investigated.

A more aggressive set of conditions were then evaluated based on high pressure H_2/air performance obtained on NASA cells. These input conditions were:

- Cathode pressure - 115 psia
- Cell temperature - 220°F
- Cell area 7.2 in^2 (1/20 Ft^2)
- Current density - 1000 ASF
- Cathode gap - .125 inches
- Air stoich - 4.0

For the above configuration and operational conditions it was determined that 1.34 in^2 of the total 7.2 in^2 of cell area would have to be devoted to humidification of the incoming air using excess H_2 side water. The analysis assumed that the exit air had to be saturated to 100% RH at 220°F, and that product water of the cell would supplement the humidification water to produce this condition. The actual relative humidity of the air entering the electrochemical active area of the cell, having passed through the humidification area, was determined to be approximately 39%. Table II, Appendix A, displays the computer analysis that sized the humidifier at 1.34 in^2. Tables III through VI show analyses at lower temperatures and pressures.

TABLE I

Computer Evaluation Results

		Case I	Case II	Case III	Case IV
Cathode Pressure	Psia	16	22	30	43
Cell Temperature	°F	165	180	200	220
Cell Area	In^2	7.2	7.2	7.2	7.2
Humidifier Area	In^2	1.02	1.02	1.02	1.02
Current Density	ASF	300	300	300	300
Cathode Gap	Inches	1/8	1/8	1/8	1/8
Air Flow	Stoich	2.5	2.5	2.5	2.5

The Appendix Tables reflect the rather complex relationships that are at work which influence the ability of the membrane to humidify the incoming air stream. In general terms the following relationships exist:

- Pressure - Increased pressure reduces required humidification
- Temperature - Increase temperature increases required humidification
- Air Flow - Increased air flow increases required humidification
- Current Density - Increased current density increases required humidification
- O_2 Gas Gap - Increased gap requires increased humidifying area
- Membrane Thickness - Increased thickness requires increased humidifying area

A "see through" acrylic model was sized from the high pressure high current density analysis. Figures 2 and 3 represent simplified drawings of the transport system subsequently employed.

In the working model the H_2 gas and humidifying water enter the bubble cavity. The H_2 becomes humidified and passes through the overflow tube into the base of the active area, where it is separated from any excess water that may have been carried with the H_2. The hydrogen is distributed across the active area by means of a gold distribution screen; inerts are removed with a bleed at the top of the active area. The excess H_2O is also removed with a bleed at the base of the active area.

A porous titanium plate in the water filled bubble cavity transmits the H_2O to the water transport portion of the membrane. This membrane carries the water to the cathode to humidify the incoming air that passes over the wet membrane.

A nitrogen-pressurized, forced liquid flow system was developed in the "see through" fixture. This system was found to be highly successful and was subsequently adopted in the test hardware. After fabrication and testing of this module based on computer analysis, the results were applied to the fabrication of actual test hardware.

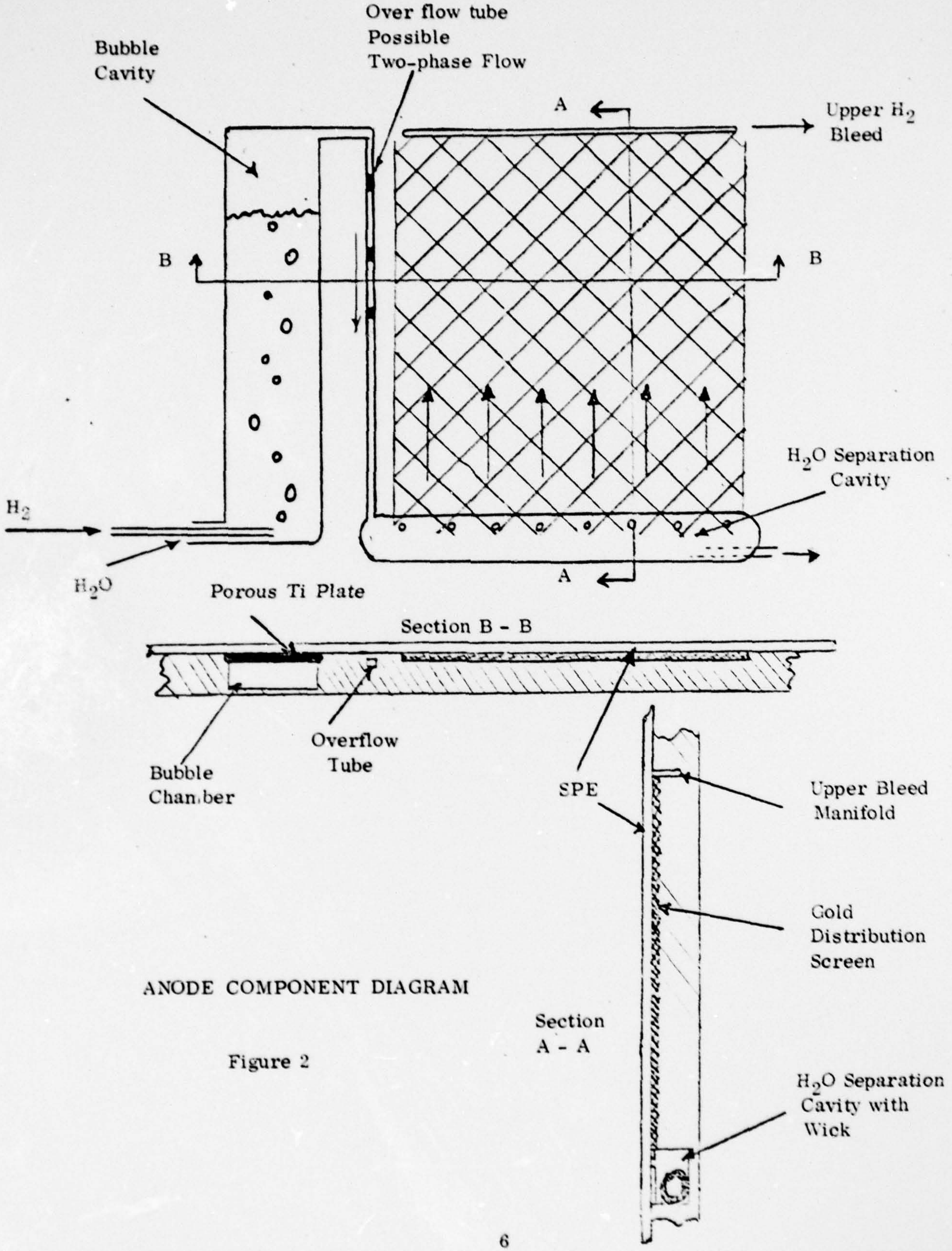

ANODE COMPONENT DIAGRAM

Figure 2

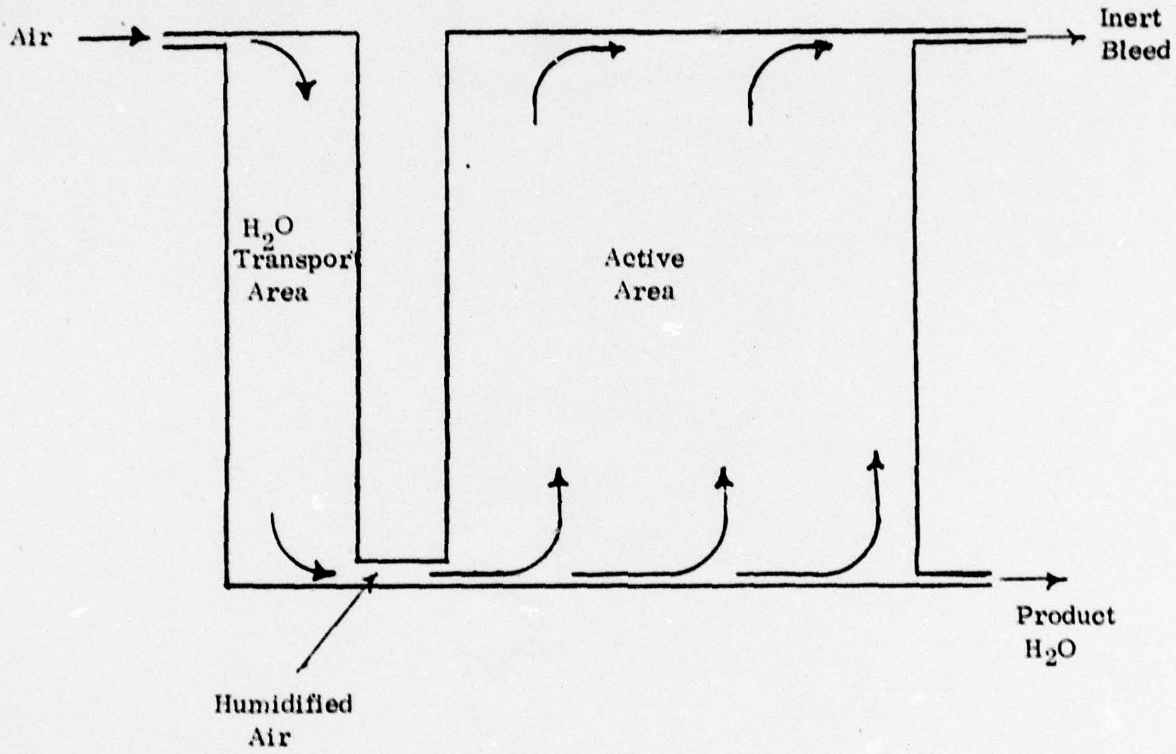

CATHODE AIR FLOW DIAGRAM

Figure 3

3.0 PARAMETRIC TESTS (Task 2.0)

Following hardware and test stand fabrication and checkout, cell M-1 was put on test. Figure 4 displays the individual cell components and Figure 5 shows the hardware integration with the test facility. M-1 was fabricated on 5 mil platinized SPE, incorporating the 4mg/cm^2 standard cathode and 4 mg/cm^2 special CO-tolerant anode catalyst (64 wt % Pt, 21 wt % Ru, 15 wt % WO_x) developed under contract to NASA/JSC (Contract NAS 9-14345). Shortly after introducing H_2O into the bubble chamber of the cell, M-1 showed signs that water was entering the anode active area, partially masking off the cell. Despite several shutdown and restart cycles this situation continued.

At this point the previously utilized "see through" fixture was set-up again to study this phenomenon. A simulation of all systems flows and pressures was imposed on this fixture and the probable cause of flooding was rapidly observed. In this hardware the water/gas mixture which spilled over the top of the anode vertical trap created a wave as the mixture flowed through the lower trap area. This wave was able to reach the gas feed parts to the active cell area. Figure 6 shows the observed two phase flow condition, as opposed to the desired condition.

With further development it was found that a woven glass wick placed in the bottom of the water seperation cavity produced the desired condition. The woven glass wick effectively interrupted the slugs so that they could be removed through the drain bleed without interfering with the active area.

Because initial testing of M-1 showed it to have less than optimum performance and higher than normal resistance, M-1 was replaced by cell M-2, which had the same configuration. The resistance of cell M-2 was also considerably higher than normal. However, the cell was activated to determine whether the water masking modifications were effective. Following activation, the reformate simulated excess water flow was set at 15 cc/hour; stable performance was maintained for two days of operation, indicating proper water distribution.

The operational temperature was increased to 165°F and a performance run on air/hydrogen was made. As shown in Figure 7, the performance demonstrated in this instance was considerably below that obtained from the NASA/JSC baseline cell. However, since the lower performance level was also obtained while operating on O_2/H_2, it appeared that the subnormal performance was not related to an inability to humidify the dry incoming air with the internal humidifier.

The higher-than-normal internal cell resistance suggested several factors that could have contributed to the low performance, including contact resistance, due to oxides on current collectors, etc., or contamination and/or oxidation of the special CO-tolerant catalyst developed for NASA/JSC.

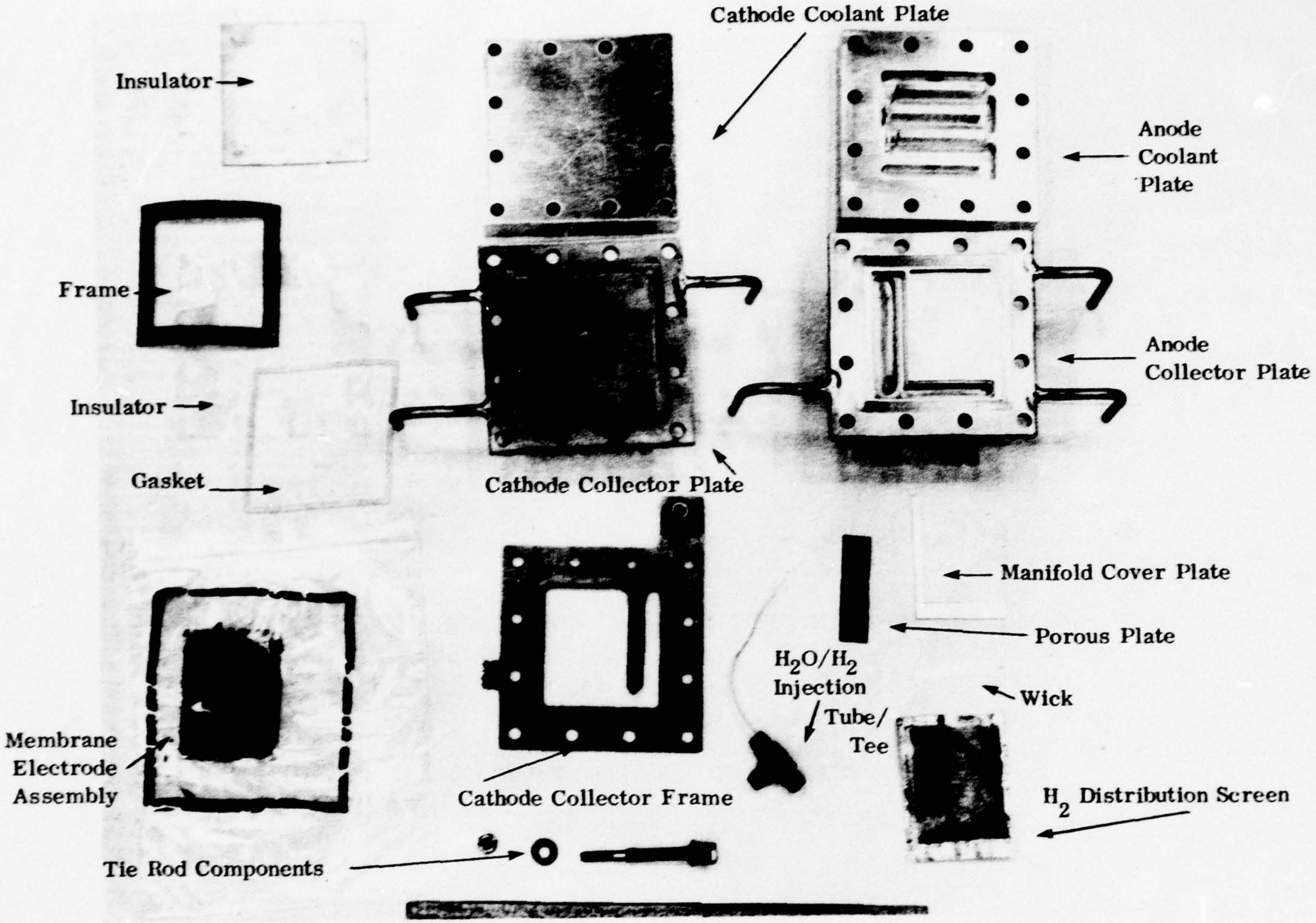

Figure 4. Reformate/Air Cell Components

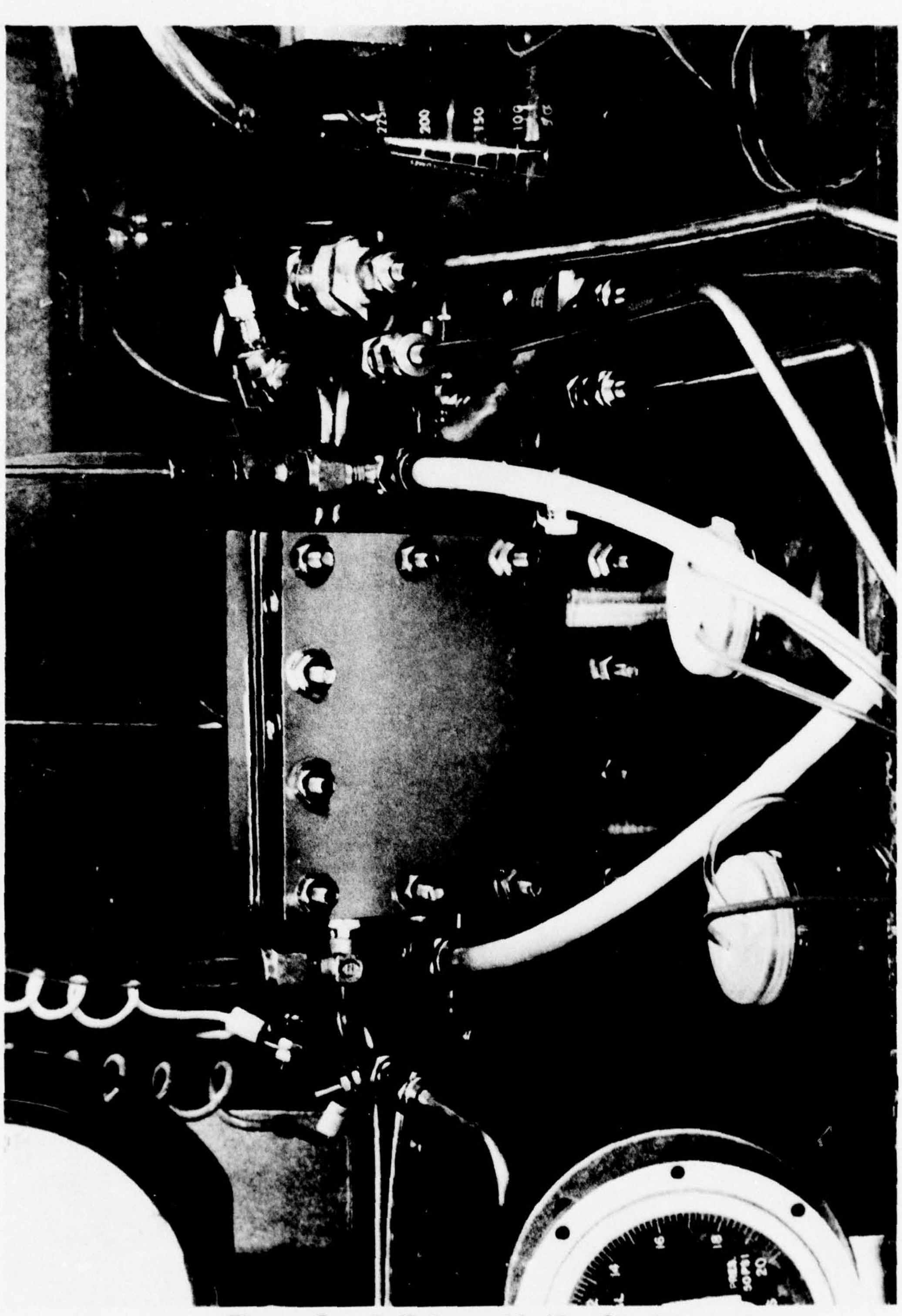

Figure 5. Cell Assembly/Facility Integration

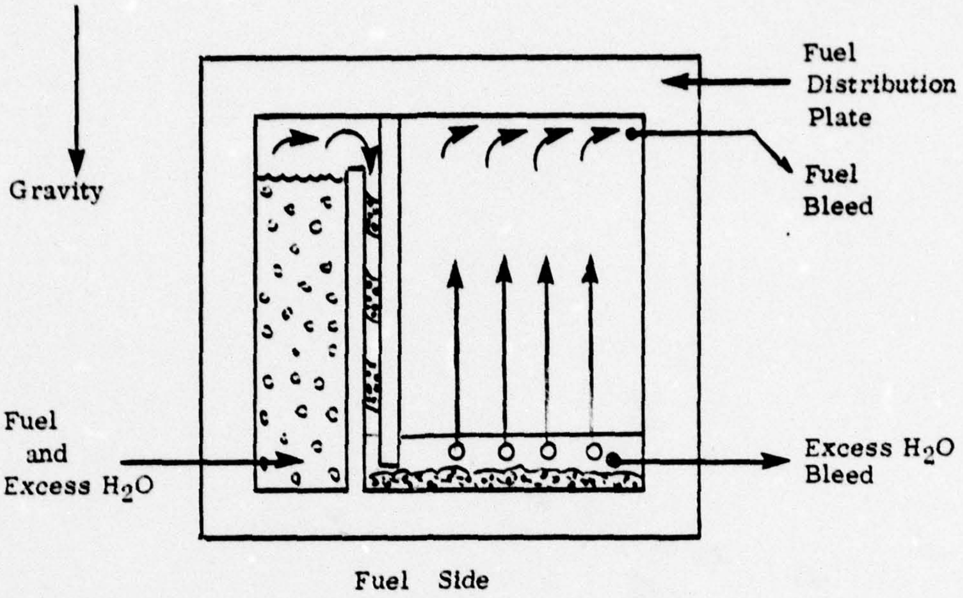

Desired Two Phase Flow

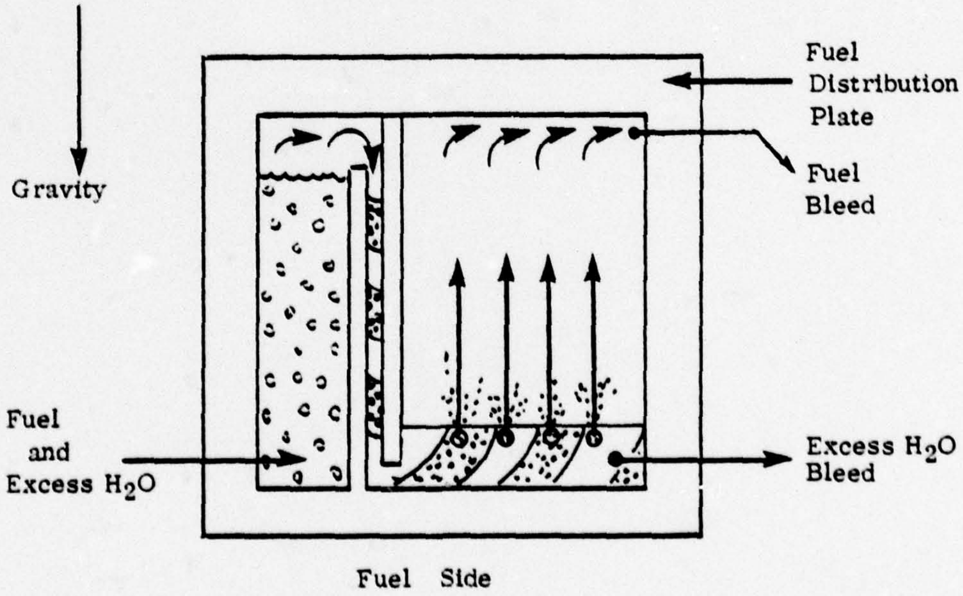

Observed Two Phase Flow

Figure 6

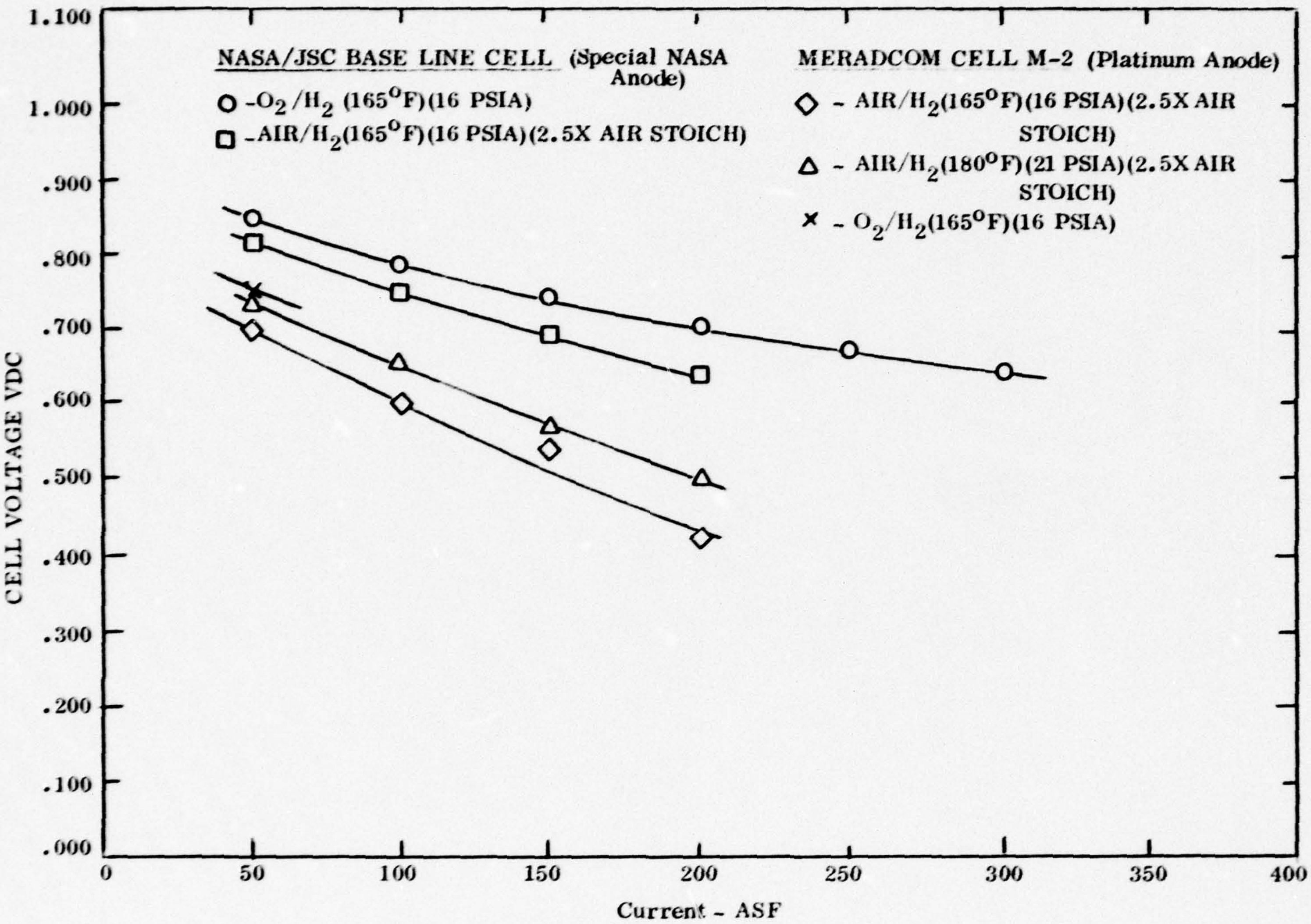

Single Cell Performance
Figure 7

The CO-tolerant catalyst used in cells M-1 and M-2 had been prepared in 1974, and subsequently not used since 1975. In view of the less than adequate performance of M-1 and M-2, it seemed possible that the batch of catalyst had undergone a negative change since it was manufactured. Preparations began for the manufacture of a new batch of the CO-tolerant catalyst. While this catalyst was being made, cells using all-platinum anodes were produced to allow further development in the interim. All cell contacts were platinum-plated to help eliminate the high internal resistance seen earlier.

Cell M-3 was the first of these all-platinum catalyst cells to go on test. Figure 8 shows performance runs on H_2/O_2 and H_2/air at 165°F and 180°F with simulated reformate excess moisture. These curves suggest significant improvement over the performance of cell M-2. At 123 hours of operation, M-3 was removed from test for analysis due to an O_2-to-H_2 leak. The analysis showed extensive blistering in the H_2O transport area.

Normally the platinization treatment of the SPE acts to prolong the life of the cell. In the H_2O transport area, however, it was believed that this treatment acted as the catalyst to produce the corrosive H_2O_2. To minimize the H_2O transport area degradation in the future, the platinization step was removed from the cell manufacturing procedure for this program.

Cell M-4 went on test shortly after the analysis of M-3; it had the same configuration as M-3 with the exception unplatinized membrane was used. Figure 9 plots the performance of M-4 at 220°F on H_2/O_2 and H_2/air at 29 psig and 100 psig.

While M-4 was being tested, the new batch of CO-tolerant catalyst was completed. Three cells were fabricated and evaluated. Although the CO-tolerant anode catalyst in these cells had been prepared by carefully following the procedure developed for NASA/JSC Houston, all three cells failed to achieve minimum performance expectations and were removed from test. Judging this new batch of catalyst to be defective, a second batch was manufactured by modifying some stock catalyst. The result effectively achieved the correct CO-tolerant mixture as developed under contract to NASA/JSC Houston. Cell M-9 was fabricated with this catalyst on unplatinized SPE with a standard platinum cathode. Figure 10 shows the O_2/H_2, Air/H_2 performance of M-9, which is significantly better than M-4, the latest previous all-platinum cell. This difference can be at least partially attributed to the cell resistances: .0052 ohms for M-9 as compared to an average resistance of .0063 ohms for M-4. Figure 11 gives performance on simulated reformate (75% H_2, 24.6% CO_2, .3% CO, .1% CH_4) /Air as a function of operating pressure. Sensitivity to fuel flow variations on simulated reformate/air is shown in Figures 12 and 13. When the performance on 10 PPM CO is compared to the performance with the .3% CO mix, the .3% CO mix showed slightly better performance at 1.25 x and 1.5 x stoichiometric flow.

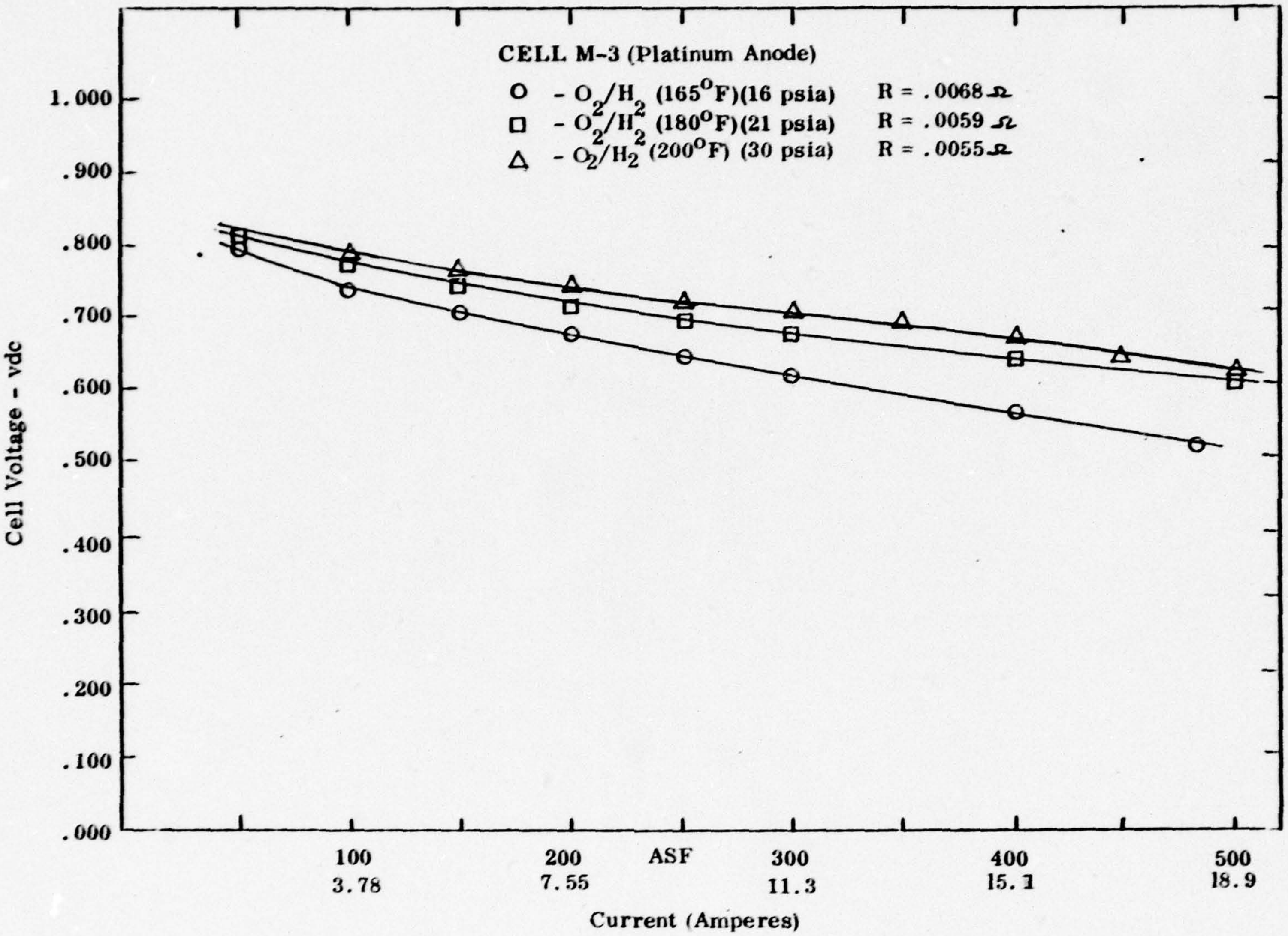

Single Cell Performance
Figure 8

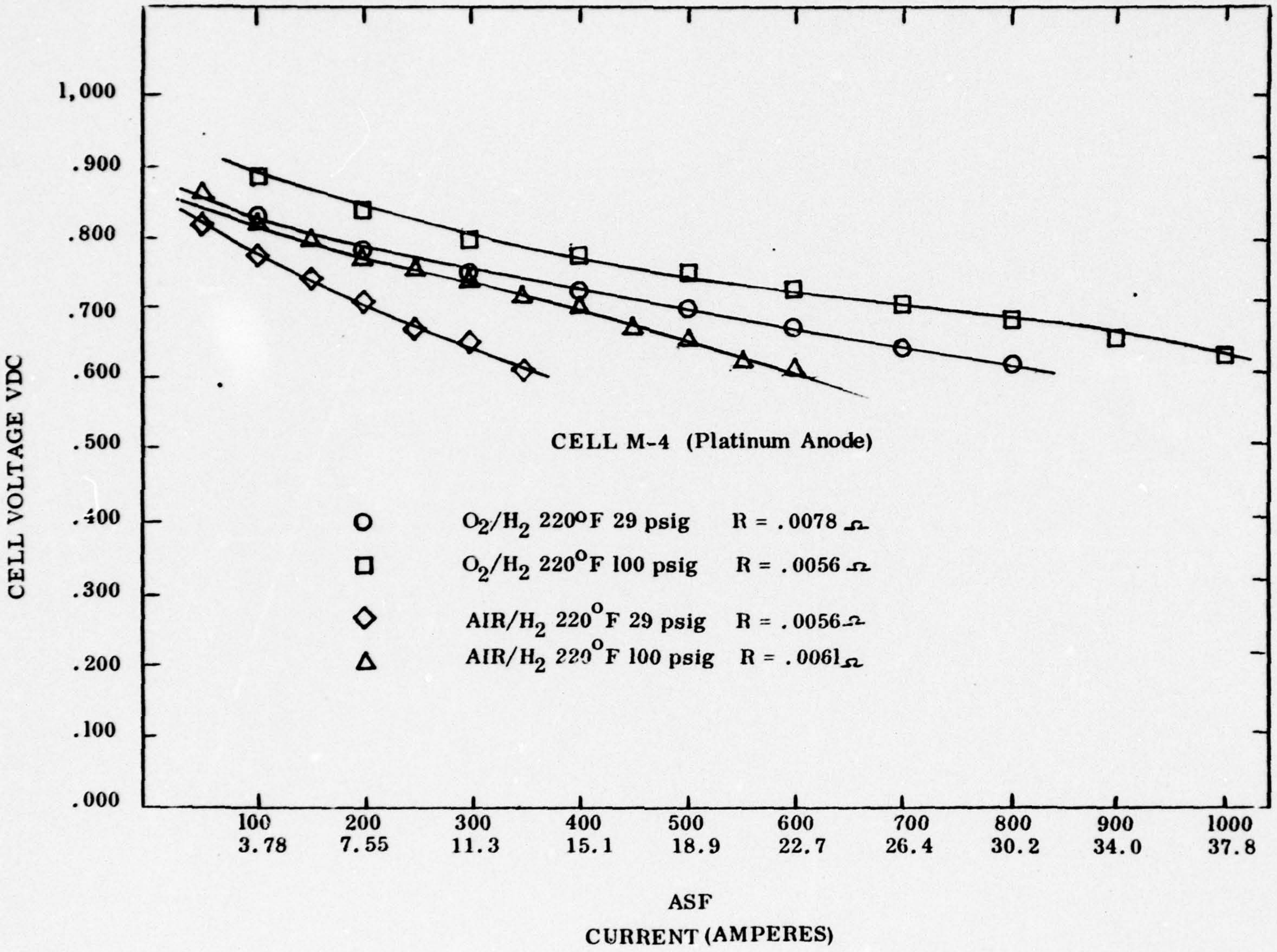

Single Cell Performance

Figure 9

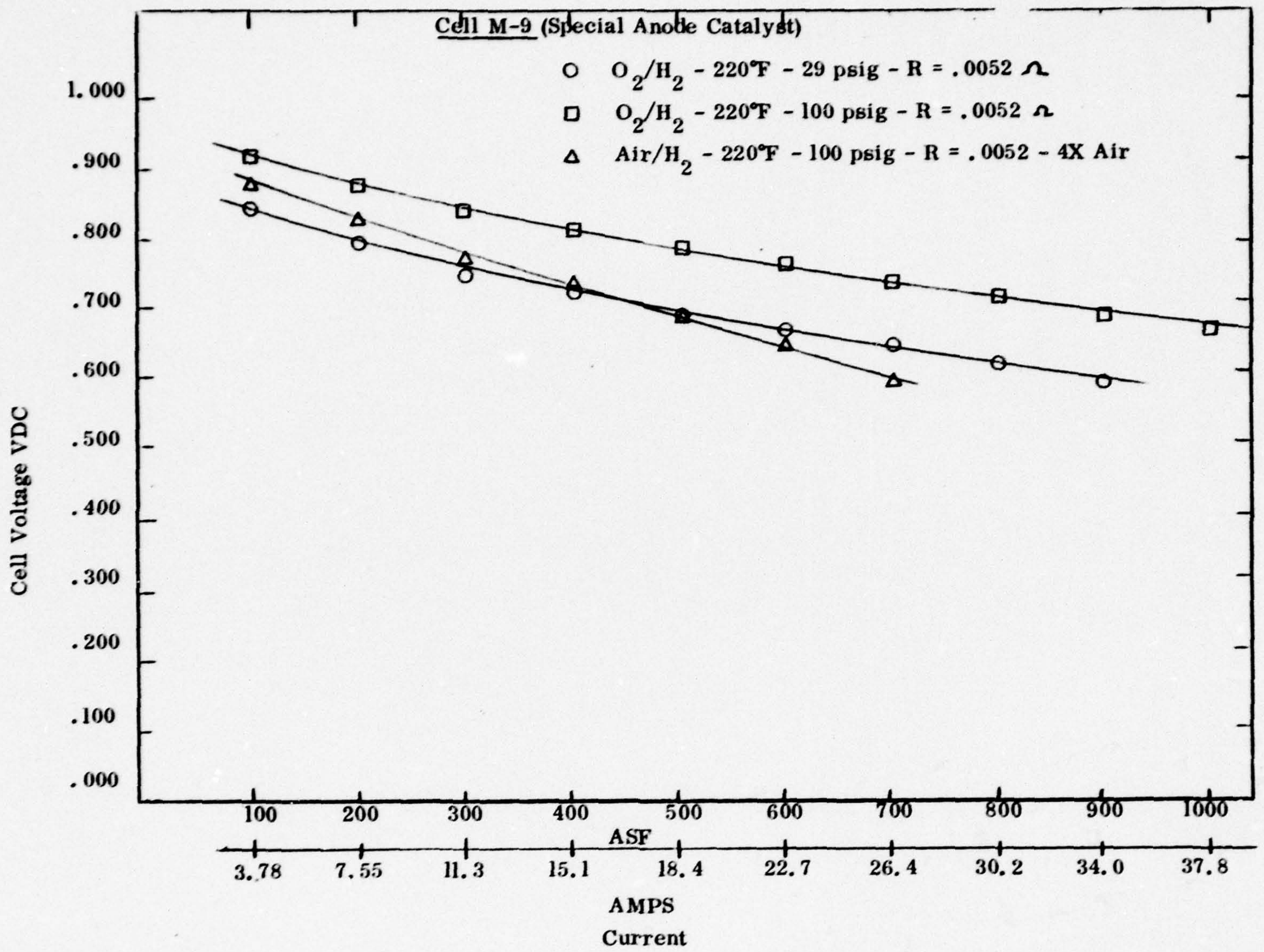
Cell M-9 (Special Anode Catalyst)
○ O_2/H_2 - 220°F - 29 psig - R = .0052 Ω
□ O_2/H_2 - 220°F - 100 psig - R = .0052 Ω
△ Air/H_2 - 220°F - 100 psig - R = .0052 - 4X Air
Cell Voltage VDC
1.000
.900
.800
.700
.600
.500
.400
.300
.200
.100
.000
100
200
300
400
500
600
700
800
900
1000
ASF
3.78
7.55
11.3
15.1
18.4
22.7
26.4
30.2
34.0
37.8
AMPS
Current

Figure 10

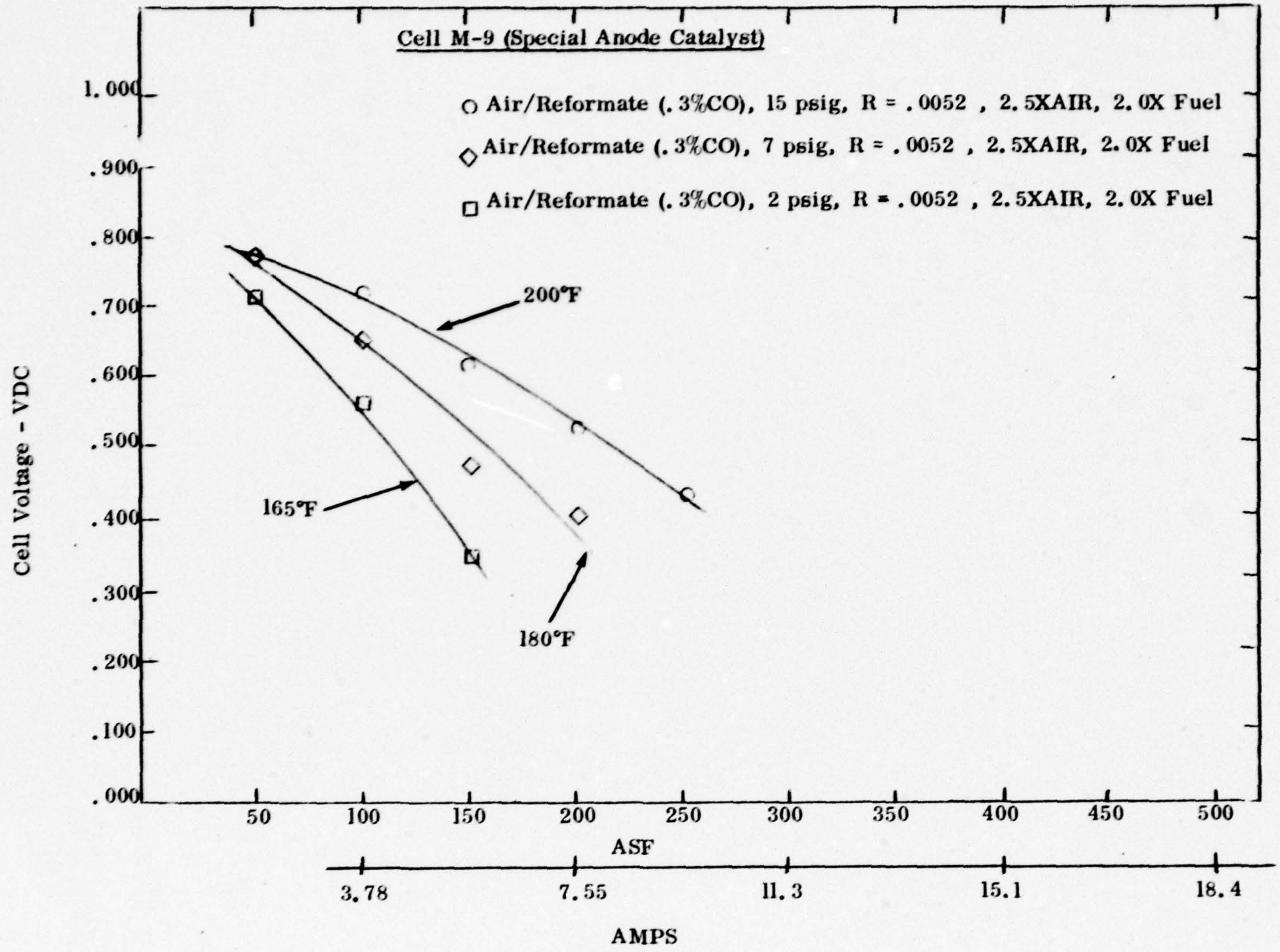

Current
Figure 11

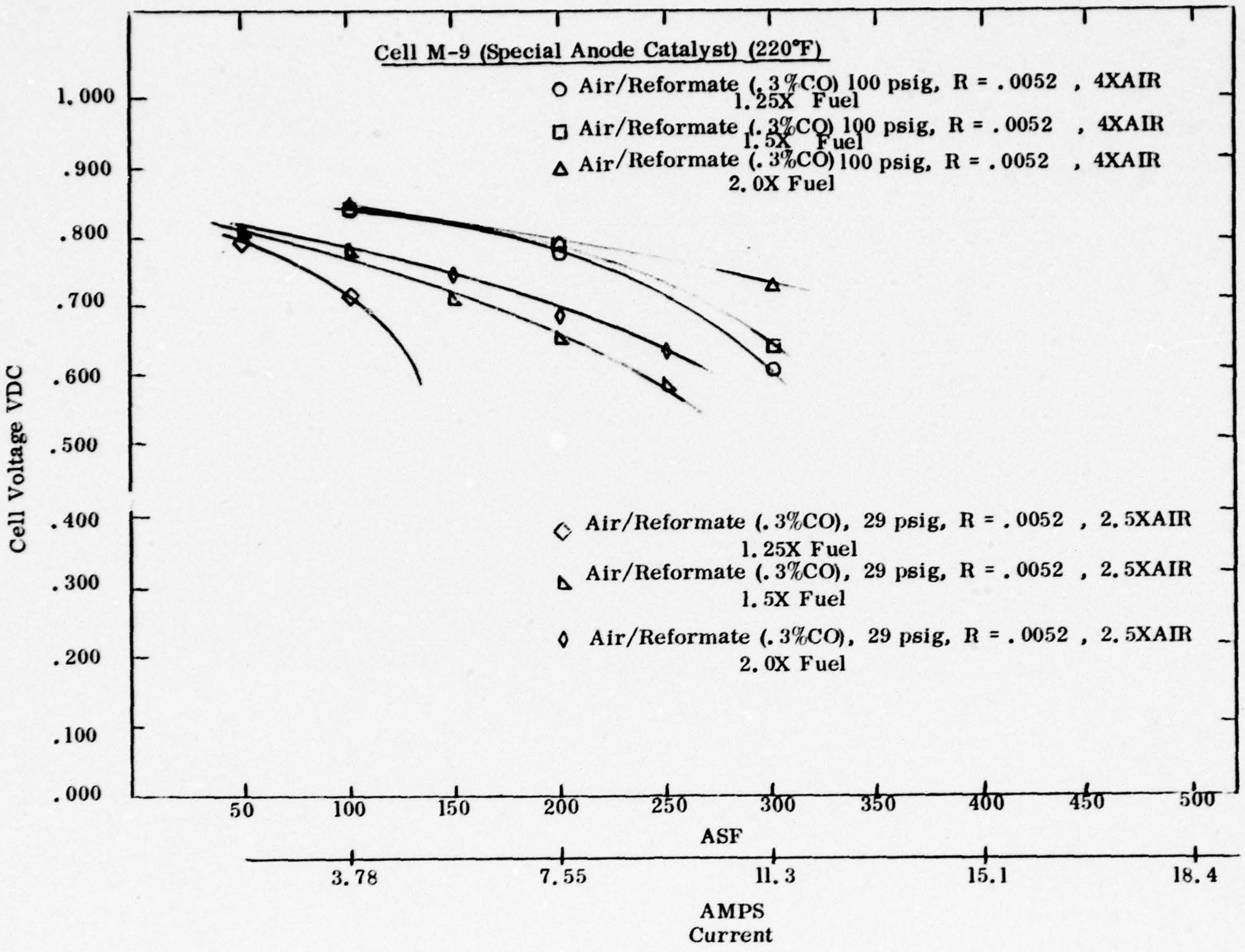
Cell M-9 (Special Anode Catalyst) (220°F)
○ Air/Reformate (.3%CO) 100 psig, R = .0052 , 4XAIR 1.25X Fuel
□ Air/Reformate (.3%CO) 100 psig, R = .0052 , 4XAIR 1.5X Fuel
△ Air/Reformate (.3%CO) 100 psig, R = .0052 , 4XAIR 2.0X Fuel
◇ Air/Reformate (.3%CO), 29 psig, R = .0052 , 2.5XAIR 1.25X Fuel
◺ Air/Reformate (.3%CO), 29 psig, R = .0052 , 2.5XAIR 1.5X Fuel
◊ Air/Reformate (.3%CO), 29 psig, R = .0052 , 2.5XAIR 2.0X Fuel
Cell Voltage VDC
1.000
.900
.800
.700
.600
.500
.400
.300
.200
.100
.000
50
100
150
200
250
300
350
400
450
500
ASF
3.78
7.55
11.3
15.1
18.4
AMPS
Current

Figure 12

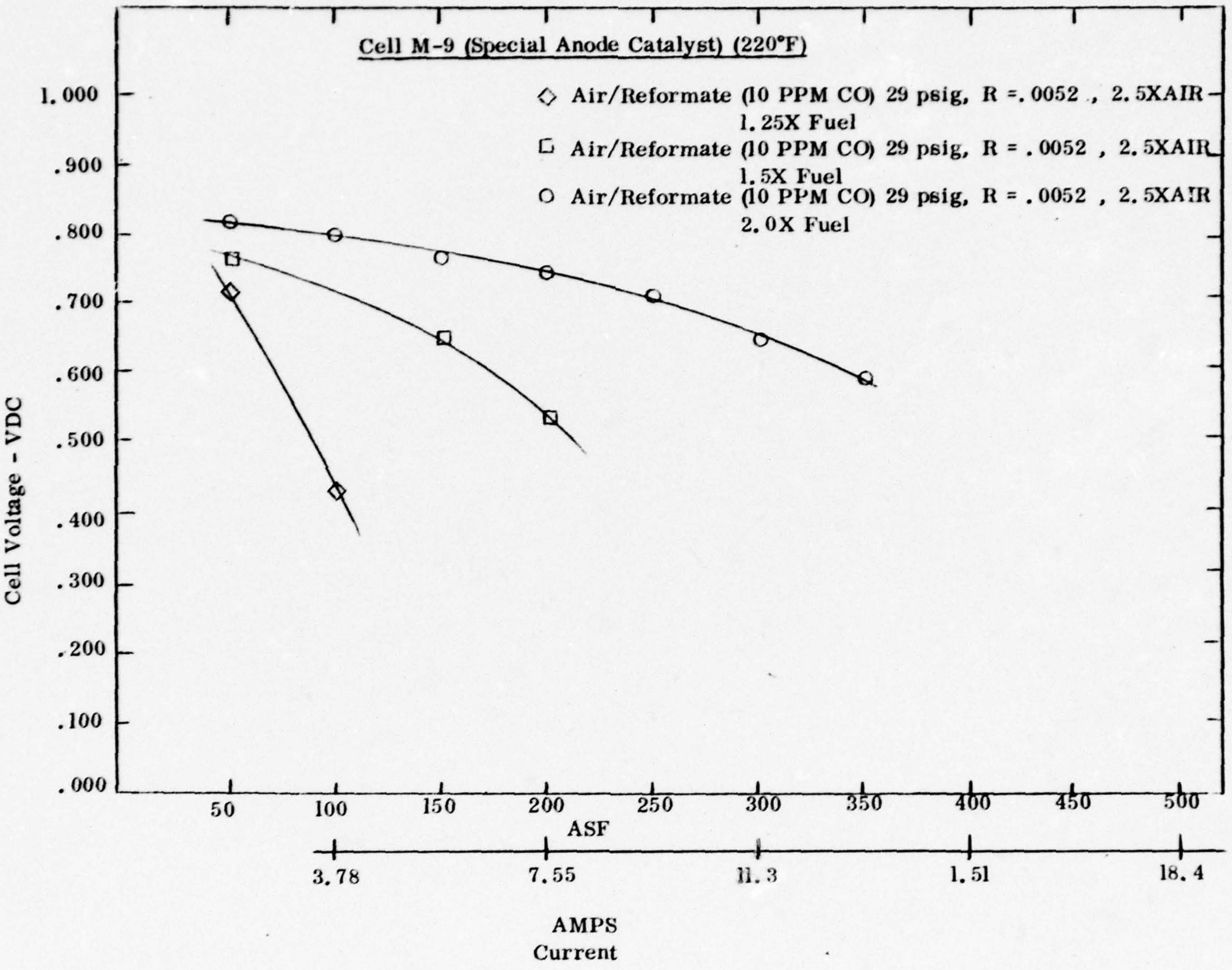
Cell M-9 (Special Anode Catalyst) (220°F)
◇ Air/Reformate (10 PPM CO) 29 psig, R =.0052 , 2.5XAIR 1.25X Fuel
□ Air/Reformate (10 PPM CO) 29 psig, R = .0052 , 2.5XAIR 1.5X Fuel
○ Air/Reformate (10 PPM CO) 29 psig, R = .0052 , 2.5XAIR 2.0X Fuel
Cell Voltage - VDC
1.000
.900
.800
.700
.600
.500
.400
.300
.200
.100
.000
50
100
150
200
250
300
350
400
450
500
ASF
3.78
7.55
11.3
1.51
18.4
AMPS
Current

Figure 13

The nature of this observation is not completely clear, however, these results suggest that there is a limited effect of the CO in the mix.

4.0 LIFE AND DURABILITY (Task 3.0)

4.1 Endurance Running

Cell M-9 began endurance on reformate (.3% CO /Air) after the completion of Task 2.0 of this program. At 295 hours of operation, M-9 experienced a cathode-to-anode leak, necessitating its removal from test. Overall visual examination of the cell showed a rust-colored stain of approximately 2 cm^2 in the H_2O transport area. A sample of this discolored area was removed and sent out for chemical analysis. Also visible was an area of membrane degradation between the H_2O transport area and the active area. A sample of the active area was also taken for chemical analysis.

The cell then underwent overall microscopic examination which detected an area of gas mixing at the base of the active area. This is believed to have been caused by H_2 entering the anode cavity during the depressurization that followed the shutdown. The membrane was finally chemically stripped of all catalyst so that the integrity of the SPE could be analyzed. Microscopic examination of the stripped SPE showed degradation between the H_2O transport area and active area only.

4.2 Load Cycle Evaluation

Cell M-11 went on test soon after the shutdown of M-9, and before the analysis of M-9 was completed. At 130 hours of load cycle operation, M-11 experienced the same fate as M-9. Cell M-11 exhibited a stain in the transport area nearly identical to that in cell M-9; however, the active area demonstrated more advanced degradation, including blistering. At this time the lab results from M-9 were returned, confirming the suspicion that the humidifying H_2O system, which is entirely of 316-SS, had contaminated the water, in turn contaminating the SPE. The chemical analysis of the stained area showed significant amounts of Ni, Fe, Al and Ti with smaller amounts of Mg. To eliminate this contamination problem, deionizers were added into the H_2O injection system of each facility and titanium tubing was installed between the deionizers and the cells. This configuration was then successfully utilized in subsequent overstress testing.

4.3 Over-Temperature Study

Facility modifications were performed and subsequently Cell M-12 went on test. Preliminary performance evaluations revealed that Cell M-12 had good initial performance (Figure 14). Temperature was increased to 266°F, and curves were made on H_2/O_2 and reformate O_2 (Figure 15). Performance on the reformate was much higher than previously experienced, and with greater stability. The sudden dip at the end of the reformate curve, and an increase in resistance,

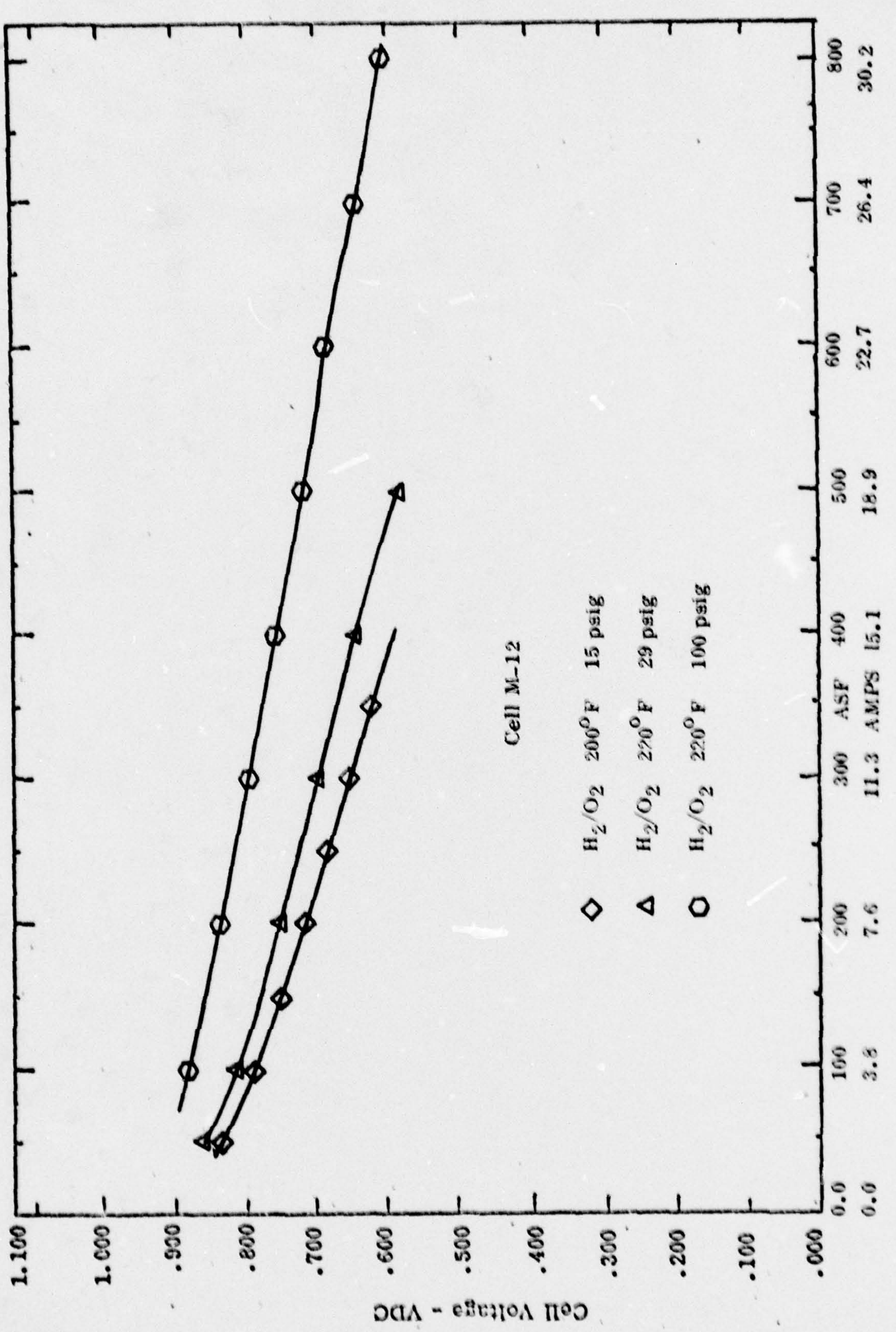
Cell M-12
◇ H_2/O_2 200°F 15 psig
△ H_2/O_2 220°F 29 psig
⬡ H_2/O_2 220°F 100 psig
Cell Voltage - VDC
1.100
1.000
.900
.800
.700
.600
.500
.400
.300
.200
.100
.000
ASF
0.0
100
200
300
400
500
600
700
800
AMPS
0.0
3.8
7.6
11.3
15.1
18.9
22.7
26.4
30.2

Figure 14

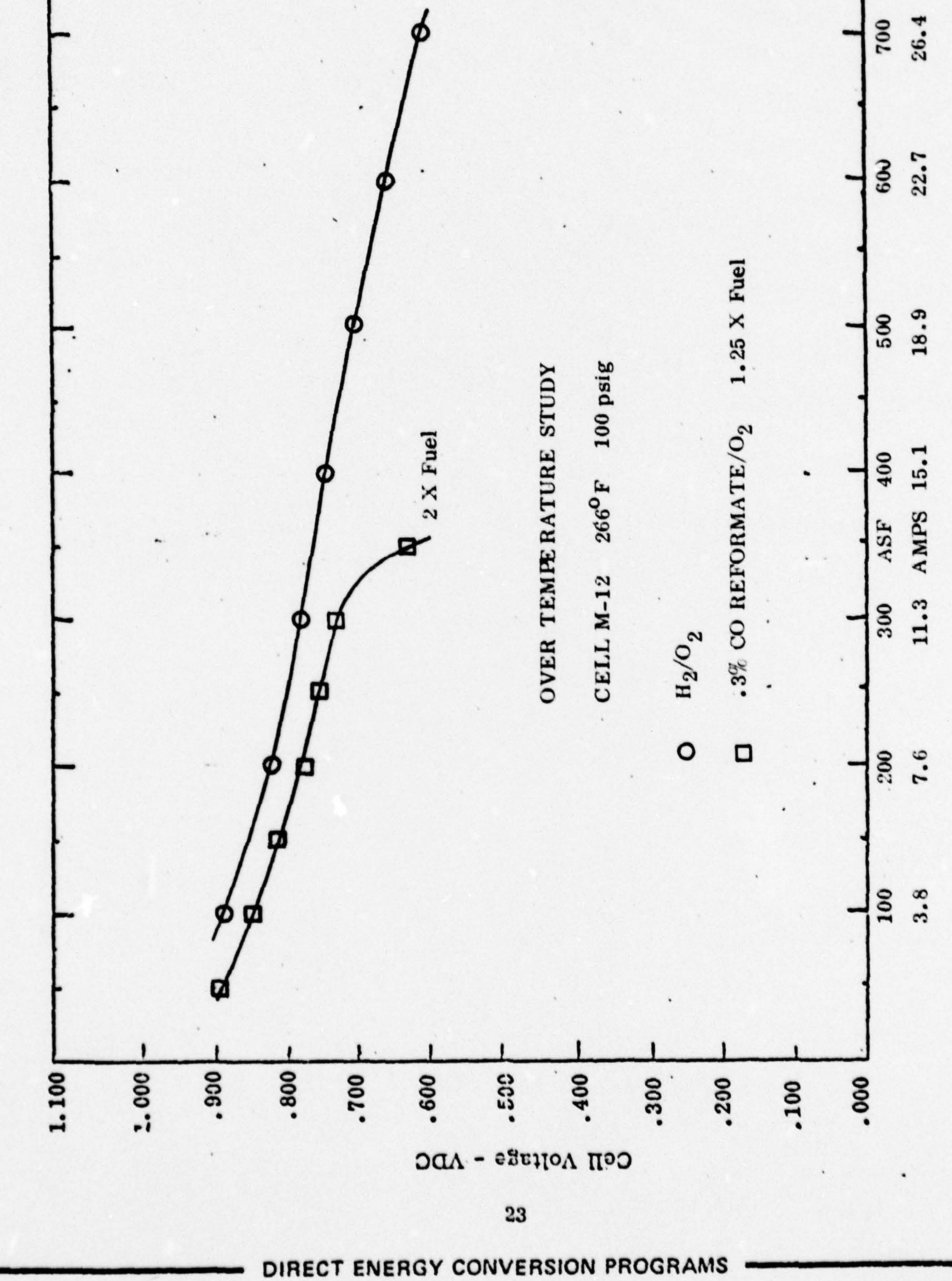
OVER TEMPERATURE STUDY
CELL M-12 266°F 100 psig
○ H_2/O_2
□ .3% CO REFORMATE/O_2 1.25 X Fuel
2 X Fuel
Cell Voltage - VDC
1.100
1.000
.900
.800
.700
.600
.500
.400
.300
.200
.100
.000
100
200
300
ASF
400
500
600
700
3.8
7.6
11.3
AMPS
15.1
18.9
22.7
26.4

Figure 15

indicated excess drying. It is believed that insufficient humidification of the high flow fuel was the cause of the performance dip and resistance increase.

4.4 Ambient Dry-Out Investigation

Cell M-11 underwent initial performance evaluations and was then removed from the test facility. The ports were left open to ambient conditions for one week. The average relative humidity during this time was 30%, with an average temperature of 68°F. M-11 was then reinstalled into the facility and activated. Figure 16 gives performance curves before and after, showing essentially no change on O_2/H_2 or H_2/Air at 220°F and 29 psig.

4.5 Freeze/Thaw Investigation

After ambient dryout testing was completed on Cell M-11 it was again removed from the facility. The ports were capped and the cell was refrigerated to -70°F (-56°C) for six hours. M-11 was allowed to thaw overnight in ambient conditions before re-activation. Performance comparisons are given in Figure 17 and reflect an increase in cell resistance. This resistance increase is believed to be the major cause for the lower performance. The cell was removed from the facility and disassembled for inspection. Visual analysis showed no obvious indications of the resistance increase. It is suspected that a minor amount of cathode detachment may have occurred.

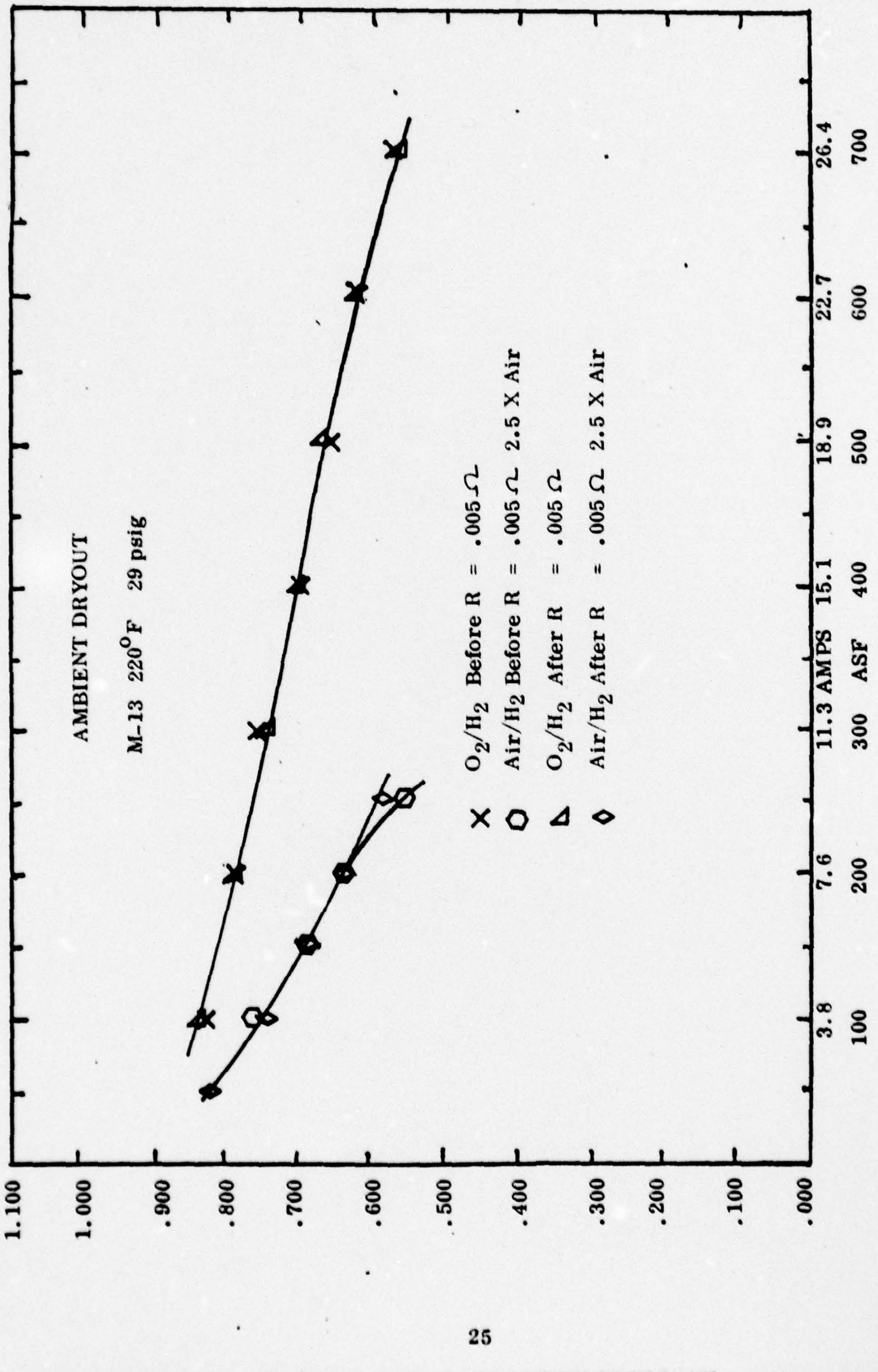
AMBIENT DRYOUT
M-13 220°F 29 psig
× O_2/H_2 Before R = .005 Ω
⬡ Air/H_2 Before R = .005 Ω 2.5 X Air
△ O_2/H_2 After R = .005 Ω
◇ Air/H_2 After R = .005 Ω 2.5 X Air
1.100
1.000
.900
.800
.700
.600
.500
.400
.300
.200
.100
.000
3.8
7.6
11.3 AMPS
15.1
18.9
22.7
26.4
100
200
300
ASF
400
500
600
700

Figure 16

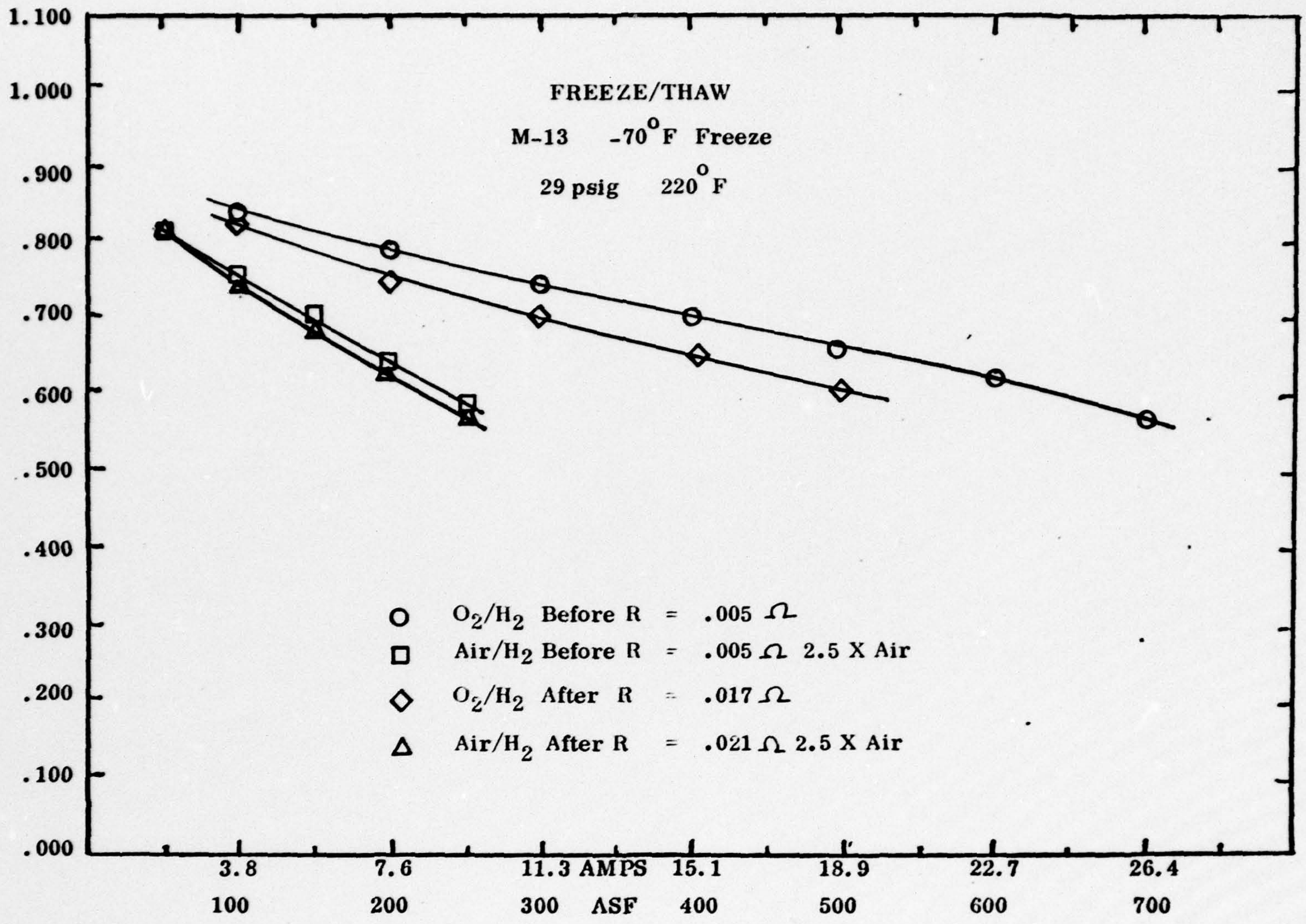
1.100
1.000
.900
.800
.700
.600
.500
.400
.300
.200
.100
.000
FREEZE/THAW
M-13 -70°F Freeze
29 psig 220°F
○ O_2/H_2 Before R = .005 Ω
□ Air/H_2 Before R = .005 Ω 2.5 X Air
◇ O_2/H_2 After R = .017 Ω
△ Air/H_2 After R = .021 Ω 2.5 X Air
3.8
7.6
11.3 AMPS
15.1
18.9
22.7
26.4
100
200
300 ASF
400
500
600
700

Figure 17

5.0 CONCLUSIONS:

The overall program results of the air/reformate fuel cell have been very enccuraging. The following conclusions/results were arrived at during the development program:

- Internal humidification of reactants was found to be successfully accomplished.
- Water carry-over to the anode active area was a correctable situation through utilization of a woven glass wick within the lower H_2 manifold.
- It was concluded that optimium humidifier performance is obtained with unplatinized SPE, thus suggesting two separate SPE's for humidification and electrical operation.
- Pre-humidification of the fuel gas (as would be the condition during use of reformate fuel) is desirable, especially at temperatures above 220° F.
- Metal ions that could contaminate the SPE should not be introduced via the excess mositure flow.
- Ambient dry-out and freezing of the hardware seems to pose little difficulty.
- Reactant flow distribution on both anode and cathode requires optimization to achieve minimum discharge flow rates.

6.0 RECOMMENDATIONS

Because the H_2O transport area requires an unplatinized SPE, and the active area has longer life with platinized hardware, configurations in the future should incorporate two different membranes: One, unplatinized, for H_2O transport, and another which is platinized for the active area.

Flow distribution studies should be performed for both anode and cathode. This is probably done best on larger scale hardware.

High temperature operation holds great potential for CO operation. However, more study is needed in this area.

Actual operation on a reformer could give further insight into an optimum design.

Recently a new SPE fuel cell technology has emerged which is superior to the open cathode gap configuration. Because this new M&E configuration uses a conductive cathode wetproofing film, axial current collection can be used instead of the interrupted wetproofing film and edge current collection used in this program. This axial current flow capability greatly simplifies multiple cell stacks and reduces the IR loss associated with edge current collection.

Because the SPE is fully supported structurally on both sides with the conductive wetproofing cell there is no sensitivity to pressure reversal, unlike the configuration used in this program. No reverse pressure sensitivity greatly improves the overall reliability of the system. In addition to these advantages the conductive wetproofing configuration would be especially applicable to the objective of this program because a much closer cathode gap is used, thus increasing the humidifying capability of the configuration tested here. The conductive wetproofing concept with its close gap also provides the opportunity for improved flow distribution within the cathode chamber. Certainly conductive wetproofing fuel cell technology should be considered in future testing and would be a considerable improvement over the cell design tested here.

An additional area of attention would be in multi-cell configurations. Presently NASA/JSC Houston is developing a 1.1 Ft^2/cell stack design utilizing conductive cathode wetproofing. This system is presently being suggested for spacecraft applications; however, terrestrial use of the design would require few modifications.

APPENDIX A

TERMINOLOGY OF APPENDIX TABLES

Computer Readout Terms

Pressure - PSIA
Temperature - ^{o}F
Area - In^2
Current Density - ASF
Current - Amps
Air Flow - Lbs/Hr
Cell Dimensions - Inches
H_2O Gen - Lbs/Hr
H_2O Loss - Lbs/Hr
Gas Gap - Inches
H_2O Evap - Lbs/Hr
RH Hum - % x 10^{-2}
Limiting SPE Evap - Lbs/Hr - Ft^2
Limiting Gas Diff - Lbs/Hr - Ft^2

Definition of the Column Readouts

Evap Area - Displayed in In^2.

RH-Gas - Displayed in % x 10^{-2}. This number provides the relative humidity of the air as it passes over the humidifier. This is an accumulative with increased area. When the RH at the end of the available humidifier area equals the difference between the water loss and generated water the loop has been closed and cell dry-out will not occur.

RH-Surf - Displayed in % x 10^{-2}. This provides the relative humidity at the evaporating surface of the membrane at various points in the humidifier/evaporator.

H_2O Flow - Displayed in Lbs/Hr. This number provides the water transport accumulation as a function of evaporation area.

Evap Rate - Displayed in Lbs/Hr - Ft^2. This number provides the evaporation rate at discrete points within the evaporation.

TABLE I
PRIMARY DESIGN DATA 220°F-115 psia

```
PRESS,TEMP,AIR STOICH,CURR DEN?115,220,4,1000
NO.STEPS,GAS GAP,EVAP WIDTH & EVAP AREA?10,.125,.5,0
NORMAL PRINT,W5 ITERATION OR R6 ITERATION(1,2 OR 3)?1
     O2 PRESS        TEMP     VAP PRESS
      115.00000  220.00020   17.18800
     CELL AREA    CURR DEN    CURRENT    AIR STOICH   AIR FLOW
        5.43707 1000.00000   37.75745     4.00000      .42942
    CELL WIDTH    CELL HT    NO.PASS    PASS WIDTH   H20 GEN     H20 LOSS
        2.68300    2.12050    3.00000      .66517      .02798       .04448
     EVAP AREA    GAS GAP   EVAP WIDTH  H20 EVAP     REL HUM
        1.34150     .12500     .50000     .01650      .38925
OXYGEN PARTIAL PRESS,PSIA     LIMITING EVAP RATES
     FC INLET    FC OUTLET    SPE EVAP   GAS DIFF
       22.69087   16.21814   11.91028    2.26779
     EVAP AREA    RH-GAS     RH-SURF    H20 FLOW   EVAP RATE
         .13415     .04932     .96463     .00198     2.12925
         .26830     .09578     .96712     .00388     2.03434
         .40245     .13957     .96939     .00569     1.94407
         .53660     .18088     .97147     .00742     1.85818
         .67075     .21989     .97337     .00908     1.77641
         .80490     .25676     .97510     .01066     1.69854
         .93905     .29162     .97670     .01217     1.62435
        1.07320     .32462     .97815     .01362     1.55366
        1.20735     .35587     .97949     .01500     1.48626
        1.34150     .38548     .98072     .01633     1.42199

VEL,FPS          DYN PRESS          REYNOLDS NO.
   .6148456          1.82361E-05      402.2566
PRESS LOSS= 3.05176E-05     PSID OR .000847 IN. H20
PRESS,TEMP,AIR STOICH,CURR DEN?STOP
```

TABLE II

165°F - 16 psia

```
PRESS,TEMP,AIR STOICH,CURR DEN?16,165,2.5,300
NO.STEPS,GAS GAP,EVAP WIDTH & EVAP AREA
?20,.0015,.125,0,1.02

     O2 PRESS       TEMP    VAP PRESS
       16.00000  165.00000     5.34000
     CELL AREA    CURR DEN    CURRENT     AIR STOICH   AIR FLOW
        5.76357  300.00000   12.00743      2.50000       .08535
    CELL WIDTH    CELL HT     NO.PASS     PASS WIDTH   H20 GEN      H20 LOSS
        2.68300    2.24033    3.00000        .70511      .00890       .02436
     EVAP AREA    GAS GAP    EVAP WIDTH  H20 EVAP     REL HUM
        1.02000     .12500     .38017       .01547       .67602
    OXYGEN PARTIAL PRESSURE,PSIA
     FC INLET   FC OUTLET
        2.59572    1.46252
     EVAP AREA     RH-GAS     RH-SURF     H20 FLOW   EVAP RATE
         .06800     .07296      .75944      .00132     2.80533
         .13600     .14638      .72987      .00274     2.98883
         .20400     .21344      .75601      .00407     2.82778
         .27200     .27365      .77949      .00534     2.67662
         .34000     .32831      .80069      .00653     2.53476
         .40800     .37810      .81974      .00767     2.40062
         .47600     .42357      .83693      .00874     2.27387
         .54400     .46521      .85247      .00976     2.15393
         .61200     .50342      .86642      .01072     2.03972
         .68000     .53855      .87909      .01163     1.93170
         .74800     .57092      .89055      .01250     1.82906
         .81600     .60080      .90103      .01331     1.73217
         .88400     .62841      .91047      .01409     1.63967
         .95200     .65395      .91888      .01482     1.55093
        1.02000     .67761      .92667      .01551     1.46757

VEL,FPS         DYN PRESS        REYNOLDS NO.
     1.16825          9.05774E-06       127.74
PRESS LOSS= 2.74181E-05    PSID OR .000761 IN. H20
```

THIS PAGE IS BEST QUALITY PRACTICABLE
FROM COPY FURNISHED TO DDC

TABLE III

180°F - 22 psia

```
PRESS,TEMP,AIR STOICH,CURR DEN?21.684,180,2.5,300
NO.STEPS,GAS GAP,EVAP WIDTH & EVAP AREA?10,10.125,0,1.02
NORMAL PRINT,WS ITERATION OR R6 ITERATION(1,2 OR 3)?1
     O2 PRESS        TEMP     VAP PRESS
       21.68400  180.00000     7.51500
     CELL AREA    CURR DEN    CURRENT    AIR STOICH   AIR FLOW
        5.76357  300.00000    12.00743     2.50000      .08535
    CELL WIDTH    CELL HT     NO.PASS    PASS WIDTH   H2O GEN     H2O LOSS
        2.68300    2.24033     3.00000      .70511      .00890      .02580
     EVAP AREA    GAS GAP    EVAP WIDTH   H2O EVAP     REL HUM
        1.02000     .12500      .38017      .01690      .69674
OXYGEN PARTIAL PRESS,PSIA      LIMITING EVAP RATES
     FC INLET    FC OUTLET    SPE EVAP    GAS DIFF
        3.44586    1.94395     6.94226     5.44807
     EVAP AREA     RH-GAS      RH-SURF     H2O FLOW   EVAP RATE
          .10200     .12619      .72597      .00243     3.42752
          .20400     .23237      .76729      .00465     3.13669
          .30600     .32273      .80189      .00669     2.87396
          .40800     .40234      .83103      .00855     2.63518
          .51000     .46751      .85569      .01026     2.41718
          .61200     .52601      .87662      .01183     2.21748
          .71400     .57723      .89443      .01328     2.03400
          .81600     .62229      .90961      .01460     1.86511
          .91800     .66207      .92255      .01581     1.70943
         1.02000     .69730      .93360      .01692     1.56585

VEL,FPS          DYN PRESS         REYNOLDS NO.
   .8847981          6.36006E-06      125.8846
PRESS LOSS= 2.09808E-05     PSID OR    .0005823 IN. H2O
```

TABLE IV

200°F - 30 psia

```
PRESS,TEMP,AIR STOICH,CURR DEN?30,200,2.5,300
NO.STEPS,GAS GAP,EVAP WIDTH & EVAP AREA?10,.125,0,1.02
NORMAL PRINT,WS ITERATION OR R6 ITERATION(1,2 OR 3)?1
      O2 PRESS        TEMP     VAP PRESS
       30.00000  200.00000    11.52900
      CELL AREA    CURR DEN    CURRENT    AIR STOICH   AIR FLOW
        5.76357  300.00000    12.00743     2.50000      .08535
     CELL WIDTH    CELL HT     NO.PASS    PASS WIDTH  H20 GEN     H20 LOSS
        2.68300    2.24033     3.00000      .70511      .00890      .03036
      EVAP AREA   GAS GAP    EVAP WIDTH  H20 EVAP    REL HUM
        1.02000     .12500      .38017     .02146      .74911
OXYGEN PARTIAL PRESS,PSIA      LIMITING EVAP RATES
      FC INLET   FC OUTLET    SPE EVAP    GAS DIFF
        4.47566     2.53417   10.39715     6.49971
      EVAP AREA     RH-GAS     RH-SURF     H20 FLOW  EVAP RATE
          .10200      .15085       .81113       .00327     4.61205
          .20400      .27219       .84724       .00620     4.14297
          .30600      .37156       .87569       .00884     3.72867
          .40800      .45411       .89833       .01122     3.36004
          .51000      .52349       .91649       .01337     3.03034
          .61200      .58236       .93112       .01531     2.73425
          .71400      .63269       .94296       .01705     2.46762
          .81600      .67601       .95256       .01863     2.22703
          .91800      .71350       .96037       .02006     2.00970
         1.02000      .74609       .96673       .02134     1.81316

VEL,FPS           DYN PRESS        REYNOLDS NO.
    .6827987          5.293915E-06     128.2382
PRESS LOSS= 1.59740E-05    PSID OR    .0004434 IN. H20
PRESS,TEMP,AIR STOICH,CURR DEN?STOP
```

TABLE V

220°F - 43 psia

```
PRESS,TEMP,AIR STOICH,CURR DEN?43.416,220,2.5,300
NO.STEPS,GAS GAP,EVAP WIDTH & EVAP AREA?10,.125,0,1.02
NORMAL PRINT,WS ITERATION OR R6 ITERATION(1,2 OR 3)?1
      O2 PRESS        TEMP     VAP PRESS
        43.41600  220.00000    17.18800
      CELL AREA    CURR DEN    CURRENT    AIR STOICH   AIR FLOW
         5.76357  300.00000    12.00743     2.50000      .08535
     CELL WIDTH    CELL HT     NO.PASS    PASS WIDTH  H2O GEN     H2O LOSS
         2.68300    2.24000     3.00000      .70511      .00896      .00137
      EVAP AREA    GAS GAP    EVAP WIDTH  H2O EVAP    REL HUM
         1.02000     .12500      .35017      .02293      .76302
OXYGEN PARTIAL PRESS,PSIA      LIMITING EVAP RATES
      FC INLET    FC OUTLET    SPE EVAP    GAS DIFF
         6.34811    3.59841    11.91028     7.36036
      EVAP AREA      RH-GAS      RH-SURF     H2O FLOW   EVAP RATE
          .10200      .16133      .82846      .00362     5.11026
          .20400      .28853      .86319      .00635     4.55107
          .30600      .39099      .88990      .00972     4.06076
          .40800      .47495      .91070      .01229     3.62962
          .51000      .54468      .92707      .01459     3.24831
          .61200      .60323      .94006      .01666     2.90967
          .71400      .65284      .95043      .01850     2.60795
          .81600      .69521      .95875      .02016     2.33855
          .91800      .73161      .96547      .02164     2.09759
         1.02000      .76305      .97090      .02298     1.88182

VEL,FPS            DYN PRESS          REYNOLDS NO.
    .4926156          .3.31937E-06      127.3689
PRESS LOSS= 1.19209E-05    PSID OR   .0003309 IN. H2O
PRESS,TEMP,AIR STOICH,CURR DEN?STOP
```

DISTRIBUTION LIST

Commander (12)
Defense Documentation Center
Cameron Station, Bldg 5
ATTN: TISIA
Alexandria, VA 22314

Chief, Research, Development & Acquisition (1)
Office, Deputy Chief of Staff
Department of the Army
Washington, DC 20310

Director (1)
Technical Information
Defense Advanced Research Projects Agency
1400 Wilson Boulevard
Arlington, VA 22209

Office of the Under Deputy Secretary (1)
of Defense (Research & Advanced Technology)
ATTN: ASST DIR, Electronics & Physical
Sciences
Washington, DC 20301

Commander (1)
Headquarters, US Army Material Development
& Readiness Command
ATTN: DRCDE-D
5001 Eisenhower Avenue
Alexandria, VA 22304

Commander (1)
US Army Electronics R&D Command
ATTN: DRSEL-KL-P
Fort Monmouth, NJ 07703

Commander (1)
US Army Transportation Research & Engineering
Command
ATTN: Research Directorate
Fort Eustis, VA 23604

Commander (1)
Harry Diamond Laboratories
DELHD-RDD (Benderly)
Adelphi, MD 20783

Chief, (1)
US Army Security Agency
Arlington Hall Station
Arlington, VA 22212

DOD Project Manager-Mobile Electric
Power (1)
ATTN: DRCPM-MEP-TM
7500 Backlick Road
Springfield, VA 22150

Technical Documents Center (2)
US Army Mobility Equipment R&D Command
ATTN: DRDME-WC
Fort Belvoir, VA 22060

Commander (1)
US Army Tank-Automotive R&D Command
Technical Library/DRDTA-UL
Warren, MI 48090

Chief (1)
Naval Ships Engineering Center
Department of the Navy
ATTN: Code 6157D, Mr. Albert Himy
Washington, DC 20362

Director, Power Branch (1)
Office of Naval Research
ATTN: 473,
800 N. Quincy Street
Arlington, VA 22217

Department of the Navy (1)
Office of Naval Research
Ballston Tower #1
Code: 472, Room 624
800 N. Quincy Street
Arlington, VA 22217

Commander (1)
Naval Ordnance Test Station
China Lake, CA 93555

Commander (1)
US Naval Electronics Laboratory
ATTN: Research Library
San Diego, CA 92152

Director (1)
US Naval Research Laboratory
ATTN: Code 2027
Washington, DC 20390

DISTRIBUTION LIST

Office of Naval Research (1)
Department of the Navy
ATTN: Code 425
800 N. Quincy Street
Arlington, VA 22217

Commanding Officer (1)
Naval Ships R&D Center
Annapolis Division
Annapolis, MD 21402

Power Information Center (1)
University City Science Center
3624 Science Center
Philadelphia, PA 19104

Commanding Officer ~~(12)~~ 10
US Army Mobility Equipment R&D Command
Electrical Power Laboratory
ATTN: DRDME-EC (Systems Group)
Fort Belvoir, VA 22060

Commander (1)
US Air Force Security Service
ATTN: DCS/Communications-
Electronics (ESO)
San Antonio, TX 78241

Commander (1)
Aerospace Power Division
ATTN: AFAPL/PO (Mr. J.D. Reams)
Wright-Patterson Air Force Base
Dayton, OH 45443

Commander (1)
Department of the Air Force (AFSC)
Rome Air Development Center
ATTN: TUGG (Mr. F.J. Mollura,3068)
Griffiss, AFB, NY 13441

Commander (1)
AFEWC (SURP)
San Antonio, TX 78241

Commander (1)
Marine Coprs Development & Education
Center
ATTN: M&L Division (M. Horstkamp)
Quantico, VA 22134

Mr. Norman Rosenberg (1)
US Department of Transportation
Transportation Systems Center
55 Broadway
Cambridge, MA 02142

US Department of Energy (1)
ATTN: Mr. Gary Voelker
20 Massachusetts Avenue, NW
Washington, DC 20545

Dr. Paul C. Milner (1)
Bell Telephone Laboratories
Murray Hill, NJ 07974

Electrochimica Corporation (1)
2485 Charleston Road
ATTN: Mr. V. Sparks, Technical Library
Mountain View, CA 94040

Engelhard Minerals & Chemical Corp (1)
Engelhard Industries Division
Government Services Department
ATTN: Mr. V.A. Forlenza
70 Wood Avenue, South
Metro Park Plaza
Iselin, NJ 08830

Exxon Research & Engineering Company (1)
PO Box 8
ATTN: Dr. G. Ciprios
Linden, NJ 07036

General Electric Company (1)
50 Fordham Road
ATTN: L.J. Nuttall, Bldg 1A
Wilmington, MA 01887

Institute of Gas Technology (1)
3434 South State Street
ATTN: Dr. K.F. Blurton
Chicago, IL 60616

Electric Power Research Institute (1)
ATTN: A.P. Fickett
PO Box 10412
Palo Alto, CA 94304

Globe-Union Inc (1)
ATTN: Corporate Research
5757 North Green Bay Avenue
Milwaukee, WI 53201

DISTRIBUTION LIST

Director (1)
George Marshall Space Flight Center
ATTN: M-ASTR-E
Huntsville, AL 38809

Director (1)
Lewis Research Center
National Aeronautics & Space Administration
ATTN: Mr. H.J. Schwartz (M.S. 309-1)
21000 Brookpark Road
Cleveland, OH 44135

Argonne National Laboratory (1)
9700 South Cass Avenue
ATTN: Dr. Paul Nelson, Bldg. 205
Argonne, IL 60439

Commanding Officer (1)
US Army Signal Warfare Laboratory
ATTN: DELSW-CC, Mr. Crabbe
Arlington Hall Station, VA 22212

Government of Canada (1)
ATTN: Mr. C.L. Gardner
2122 Rushton Road
Ottawa, Ontario, Canada KZA1N7

Gas Research Institute (1)
ATTN: Dr. Lloyd R. Lawrence, Jr.
3424 South State Street
Chicago, ILL 60616

Dr. Ralph Roberts (1)
Energy Resources & Environmental Systems Engineering
The MITRE Corporation
Mail Stop W-389
Westgate Research Park
McLean, VA 22101

Universal Oil Products, Inc. (1)
Ten UOP Plaza
ATTN: Stephen N. Massie
Government Contract Administrator
Des Plaines, IL 60016

Technology Center (1)
ESB Incorporated
19 W. College Avenue
ATTN: Dr. D.T. Ferrell, Jr.
Yardley, PA 19067

Power Systems Division (1)
United Technologies Corporation
ATTN: Mr. Al Meyer
PO Box 109, Governor's Highway
South Windsor, CT 06074

Union Carbide Corporation (1)
Parma Research Center
PO Box 6166
ATTN: Dr. R. Brodd
Parma, OH 44101

Dr. S.B. Brummer (1)
Director of Physical Research
EIC, Inc.
55 Chapel Street
Newton, MA 02158

Shell Development Company (1)
ATTN: Dr. D.C. Olson
PO Box 262
Wood River, ILL 62095

IIT Research Institute (1)
ATTN: Mr. Edward Fochtman
10 West 35th Street
Chicago, IL 60616

Dr. P. Stonehart (1)
Stonehart Associates, Inc.
34 Five Fields Road
Madison, CT 06443

Jet Propulsion Laboratory (1)
California Institute of Technology
ATTN: Dr. John Houseman, Supervisor
Fuel Conversion Group
4800 Oak Drive
Pasadena, CA 91103

Massachusetts Institute of Technology (1)
ATTN: Professor H.P. Meissner
Cambridge, MA 02138

U.C.L.A. (1)
Department of Chemical Engineering
ATTN: Prof. D. Bennion
Los Angeles, CA 90007

Institue of Defense Analysis (1)
400 Army-Navy Dirve
Arlington, VA 22202

DISTRIBUTION LIST

Director (1)
National Aeronautics & Space Administration
ATTN: Code RPP, Mr. A. Dan Schnyer
Washington, DC 20546

Energy Research Corporation (1)
ATTN: Dr. B. Baker
3 Great Pasture Road
Danbury, CT 06810

University of Wisconsin (1)
Department of Chemical Engineering
ATTN: Professor S. H. Langer
Madison, WI 53706